Nanomaterials via Laser Ablation/Irradiation in Liquid: A Review

Haibo Zeng, Xi-Wen Du,* Subhash C. Singh,* Sergei A. Kulinich,* Shikuan Yang, Jianping He, and Weiping Cai*

Laser ablation of solid targets in the liquid medium can be realized to fabricate nanostructures with various compositions (metals, alloys, oxides, carbides, hydroxides, etc.) and morphologies (nanoparticles, nanocubes, nanorods, nanocomposites, etc.). At the same time, the post laser irradiation of suspended nanomaterials can be applied to further modify their size, shape, and composition. Such fabrication and modification of nanomaterials in liquid based on laser irradiation has become a rapidly growing field. Compared to other, typically chemical, methods, laser ablation/irradiation in liquid (LAL) is a simple and "green" technique that normally operates in water or organic liquids under ambient conditions. Recently, the LAL has been elaborately developed to prepare a series of nanomaterials with special morphologies, microstructures and phases, and to achieve one-step formation of various functionalized nanostructures in the pursuit of novel properties and applications in optics, display, detection, and biological fields. The formation mechanisms and synthetic strategies based on LAL are systematically analyzed and the reported nanostructures derived from the unique characteristics of LAL are highlighted along with a review of their applications and future challenges.

1. Introduction

In 1960, Maiman constructed the first functional laser at Hughes Research Laboratories.[1] From then on, lasers have been widely used in a range of science and technological fields, among which the laser-assisted fabrication of functional materials is undoubtedly one of the most significant applications.

The ablation of the target material upon laser irradiation is a very complex process. The incident laser pulse penetrates into the surface of the material within a certain penetration depth. This dimension is dependent on the laser wavelength and the refraction index of the target material and is typically in the range of 10 nm. The strong electrical field generated by the laser light is sufficient to remove electrons from the bulk of the penetrated volume within 10 ps for a nanosecond laser pulse.[2] The free electrons oscillate within the electromagnetic field and can collide with the atoms of the bulk material, thus transferring some energy to the lattice. The irradiated surface is then heated up and vaporized.[2] At a high enough laser flux, the material is typically converted to plasma, as shown in **Figure 1**a, which contains various energetic species including atoms, molecules, electrons, ions, clusters, particulates, and molten globules, and therefore possesses some unique characteristics such as high temperature, high pressure, and high density.[3] Subsequently, the large pressure difference between the laser produced initial seed plasma and ambient atmosphere causes a rapid expansion of the plasma plume and then it cools down. This process is

Prof. H. B. Zeng, Dr. S. K. Yang, Prof. J. P. He
Key Laboratory for Intelligent Nano Materials and Devices of the Ministry of Education
State Key Laboratory of Mechanics and Control of Mechanical Structures
College of Material Science and Technology
Nanjing University of Aeronautics and Astronautics
Nanjing 210016, China
E-mail: zeng.haibo.nano@gmail.com
Prof. H. B. Zeng, Prof. W. P. Cai
Key Laboratory of Materials Physics,
Anhui Key Laboratory of Nanomaterials and Nanotechnology
Institute of Solid State Physics
Chinese Academy of Sciences
Hefei 230031, China

DOI: 10.1002/adfm.201102295

Prof. X.-W. Du
School of Materials Science and Engineering
Tianjin University
Tianjin 300072, China
E-mail: xwdu@tju.edu.cn
Dr. S. C. Singh
National Centre for Plasma Science and Technology (NCPST) School of Physical Sciences
Dublin City University
Glasvevin, Dublin-9, Ireland
E-mail: subhash.singh@dcu.ie
Dr. S. A. Kulinich
Graduate School of Engineering,
Center for Atomic and Molecular Technologies
Osaka University
Osaka 565-0871, Japan
E-mail: s_kulinich@yahoo.com

nearly adiabatic and transsonic.[3] Under suitable condensation conditions (temperature and pressure), the plasma species will nucleate and grow into desirable nanostructures, either on a substrate or in a cool liquid medium.

The laser-target interaction can be designed in different environments to fabricate various materials. Most conventionally, beginning in 1965, it has been applied in vacuum chambers to fabricate thin films, with the technique being referred to as pulsed laser deposition (PLD),[4] as shown in Figure 1b. In this method, the material is vaporized from the target in ultrahigh vacuum or in the presence of a background gas to form a plasma plume, which is then deposited as a thin film on a substrate. The technique of PLD has been successfully applied to fabricate a series of thin films with high crystalline quality, including ceramic oxides, nitrides, metallic multilayers, and various superlattices, as well as polycrystalline or single-crystal films with different textures.[5] Compared with other methods, PLD demonstrates relatively lower costs than, e.g., molecular beam epitaxy (MBE) and metal-organic chemical vapor deposition (MOCVD), but generally allows the preparation of films with higher crystalline quality than most of the other methods.

In the past two decades, with the rise of nanoscience, laser ablation (LA) has been broadly applied and developed for the synthesis of nanostructures. The LA synthesis of nanomaterials can take place in two distinct environments: in a vacuum, or gaseous, environment or in a liquid medium. For the former, LA is usually combined with a tube furnace or vacuum chamber, as shown in Figure 1a–c. The combined tube furnace can provide good control over the growth temperature, flowing gas type, rate, and pressure. Such a configuration, so-called pulsed laser ablation (PLA), combines the advantages of both laser and furnace, especially in the synthesis of 1D nanomaterials, such as nanowires and nanotubes. First, due to the high energy flux of the laser spot, almost any materials can be ablated for the synthesis purpose. In addition, the PLA can generally allow better control over stoichiometry and phase composition, which is very advantageous for the growth of complex materials, including some high-quality nanomaterials that are difficult to prepare otherwise. The PLA has been applied to prepare nanowires of Si and Ge,[6] binary (In_2O_3,[7] SnO_2,[8] ZnO,[9] Zn_3P_2[10]) and ternary ($GaAs_{0.6}P_{0.4}$, $InAs_{0.5}P_{0.5}$, CdS_xSe_{1-x}, indium tin oxide (ITO))[11,12] compounds, and more complex materials.[13] Moreover, it has also been used to grow doped nanowires,[14] as well as block-by-block superlattice nanowires.[15] Holmes et al.[16] produced several-micrometer-long and defect-free Si nanowires with diameters in the range of 4–5 nm using a supercritical fluid solution phase approach. Silicon atoms were dissolved in sterically stabilized Au nanoparticles (NPs) until reaching supersaturation, at which point they were expelled from the particles in the form of thin nanowires. Several researchers reported Au nanodroplets by gas phase PLA of Au target in the presence of gaseous precursors such as silane at high temperatures to generate 1D nanostructures.[17] Duan and Lieber employed gas phase PLA of composite targets made of galium nitride (GaN) powder and catalytic metals to generate liquid nanoclusters, which served as reactive sites for the confinement and determination of direction for the growth of crystalline GaN nanowires.[18] A recent report by Singh and Zeng briefly reviews the current state of the art in the field for various laser-based processing routes for NPs and nanopatterns.[19]

Haibo Zeng received his Ph.D. degree in Condensed Matter Physics from the Chinese Academy of Sciences (CAS) in 2006, then worked in at the CAS, the Universität Karlsruhe (Germany), and the National Institute for Materials Science (Japan). In 2011, he joined Nanjing University of Aeronautics and Astronautics. His current research focuses on semiconducting 2D crystals, alloyed ZnO nanomaterials, and their applications in photodetectors, supercapacitors, and solar cells.

Xi-Wen Du received his Ph.D. in Materials Physics and Chemistry from Tsinghua University in 2001, then worked at the Motorola Company and the National Institute for Materials Science (Japan). He was then appointed Associate Professor at Tianjin University in 2003 and promoted to Full Professor in 2007. He leads the research group for quantum-dot materials and devices.

Subhash C. Singh received his Ph.D. from the University of Allahabad, India, and is working as an IRCSET-EMPOWER postdoctoral fellow at the National Centre for Plasma Science and Technology, Dublin City University, Ireland. His current research interests include laser–matter interactions and plasma processing, laser-induced nanoparticle synthesis and modification, and materials for energy harvesting and storage.

It was less than two decades ago that laser ablation was firstly implemented in liquid media (laser ablation in liquid (LAL)) to fabricate a colloidal solution of nanoparticles, as shown in Figure 1d. In 1993, Henglein and Cotton applied a pulsed laser to ablate pure metal targets in various solvents to form colloidal solutions containing metal NPs.[20,21] Since then, LAL has been developed into an important method to prepare metal, semiconductor, and even polymer NPs. As a technique, LAL is somewhat different from the other laser ablation approaches that operate in vacuum or gaseous environments because the liquid

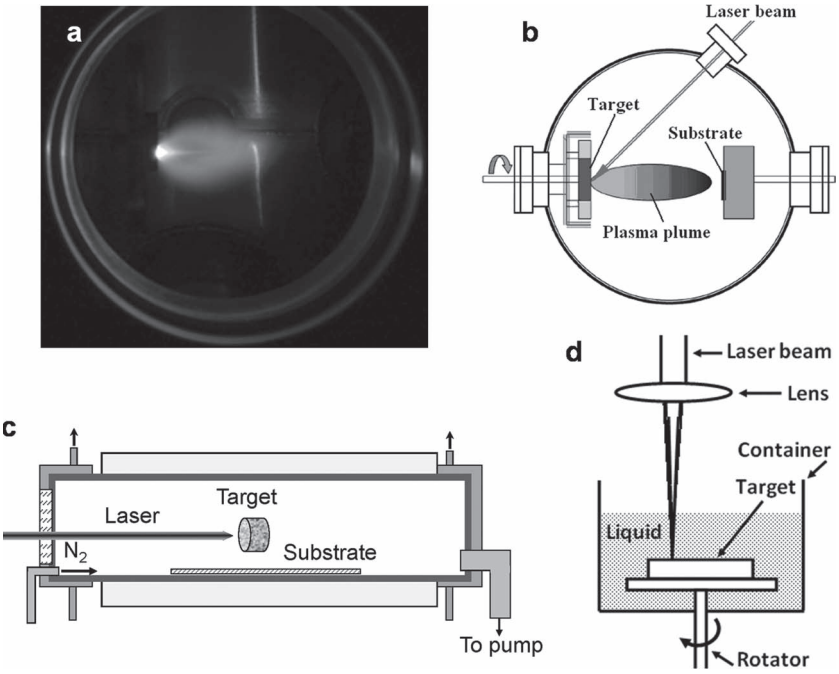

Figure 1. a) A plasma plume ejected from a laser-irradiated $SrRuO_3$ target. b) Schematic setup of pulsed laser deposition (PLD) in a vacuum chamber for thin film growth. c) pulsed laser ablation (PLA) in a tube furnace for nanowire/nanotube growth. d) LAL setup for nanoparticle growth.

medium not only provides some effective controlling parameters for fabrication, but also greatly affects the morphology and microstructure of the products. Indeed, interesting shape and size modifications of NPs prepared by laser post irradiation have been observed. The amazing prospects emerging from the interaction of matter with light have inspired numerous research groups to focus their work on the laser generation and modification of NPs in liquid and on the properties and applications of the LAL-formed NPs.

According to the results reported thus far, LAL is a simple and versatile method to synthesize various NPs. Early studies mainly focused on two subjects: i) the preparation of NPs via laser ablation of (mainly noble) metal targets[22–29] and ii) the modification of the NP size and shape.[30–35] In the past five years, in addition to the conventional synthesis of metal NPs, one trend that should be noticed is that researchers have started to adequately use the unique features of LAL to fabricate various nanostructures with novel morphologies,[36–39] microstructures, and phases,[40–43] which makes it possible to explore novel properties and applications for the new products, such as excellent biodetection[43–46] and controllable luminescence.[47–50] However, up to now, there is not a review concerning these recent important progress.

This article by no means aims at providing comprehensive information on nanomaterials prepared using the LAL technique. Instead, it focuses on describing the status of research on their formation mechanisms, modification, properties, and applications. After an introduction to the origin and brief history of the method, the second section describes the reported mechanisms involved into nanostructure generation and/or modification via laser treatment in liquid. In the third section, we address, in detail, all known methodologies within the LAL. The fourth section lists the achieved products with an emphasis on the recently reported nanostructures with novel morphologies and phases. Then, we mention and discuss the progress in the applications of various nanostructures prepared via LAL. Finally, conclusions are drawn and an outlook is presented.

2. Mechanisms Involved in LAL

2.1. LAL Mechanisms for Bulk Metal Targets

When a laser beam heats the metal target, plasma, vapor, and metal micro- or nanosized droplets can be generated as possible initial products, which further react with the liquid medium to form NPs.[51–55] Among the three possible products, the vapor and plasma can be generated by using short pulse-width lasers with high-energy density,[52,56–58] e.g., nanosecond pulsed laser with a pulse width of several nanoseconds and power density of 10^8 to 10^{10} W cm^{-2}.[52,59,60] Meanwhile, nanodroplets were reported to be the main product when low-power density lasers (e.g., millisecond lasers) were used.[36–39] So far, the main formation mechanisms of laser ablated nanostructures were based on i) the thermal evaporation (and thus formation of the vapor or plasma phase) with the subsequent interactions with the liquid and ii) the explosive ejection of nanodroplets.[36–39,59–61]

2.1.1. Thermal Evaporation Mechanism

For the thermal evaporation mechanism, Zeng and coworkers[48,59–61] performed a detailed investigation of the laser ablation of Zn, Fe, and Si targets in water by using a neodymium-doped yttrium aluminium garnet (Nd:YAG) pulsed laser (wavelength 1064 nm, frequency 10 Hz, pulse duration 10 ns) with a power of ≈80 mJ per pulse and a spot size ≈2 mm in diameter (on the target). The formation of nanostructures was attributed to the combination of ultrafast quenching of a hot plasma and its interaction with the surrounding medium.[59] In the case of a solid target, such as a Fe target (**Figure 2**), a high-temperature and high-pressure Fe plasma was reported to be produced at the solid/liquid interface after the very first pulsed-laser shot, and the subsequent ultrasonic adiabatic expansion of the hot plasma led to a quick cooling of the plume region, and hence to the formation of Fe clusters. The as-formed Fe clusters interacted with the surrounding aqueous solution, resulting in the formation of final FeO NPs. Additionally, many kinds of oxide and hydroxide NPs were fabricated using this mechanism.[62,63]

Yang et al.[52,62] also used a Nd:YAG laser (532 nm, pulse duration 10 ns, power density 1010 W cm^{-2}) and proposed another thermal evaporation model in which two types of

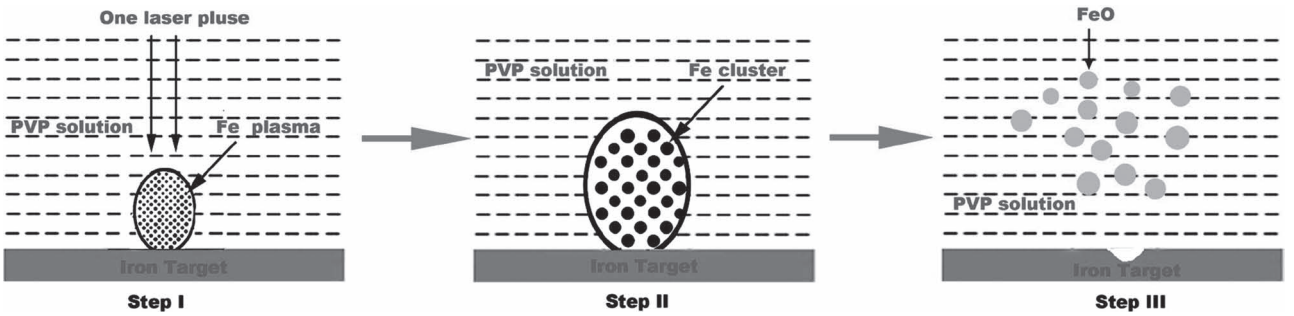

Figure 2. Schematic illustration of the formation of FeO NPs by LAL. Step I: Production of high-temperature and high-pressure iron plasma above the iron target quickly after one laser pulse. Step II: Ultrasonic and adiabatic expansion of the plasma and formation of iron clusters. Step III: Formation of ferrous oxide NPs. Reproduced with permission.[48] Copyright 2005, American Chemical Society.

plasma, i.e., a laser-induced one from the target and a plasma-induced plasma from the liquid medium, are involved. After a laser shot on the target, the target was proposed to be heated and evaporate to a plasma state, and the plasma was then excited and evaporated the surrounding liquid, turning it to plasma. The two above plasmas were reported to mix and react, eventually cooling down and condensing with the production of compound NPs.[52,62]

Yang presented a comprehensive review on PLA in liquid for the generation of NPs, in which various fundamental aspects of the technique (such as liquid confinement, thermodynamic and kinetic aspects, as well as physical and chemical aspects) were described.[52] In another report, Simakin and co-workers described PLA of Ag and Au noble metals in different liquids at various laser irradiances to prepare metallic NPs.[59] They also reported the synthesis of β-Ti, TiC, and TiO_x NPs via PLA of Ti in ethanol, dichloroethane, and water, respectively, while the irradiation of a mixture of colloidal solutions of PLA produced Ag and Au NPs led to the preparation of Ag-Au alloy NPs.[59]

2.1.2. Explosive Ejection Mechanism

Another mechanism, the explosive ejection model, was proposed to explain the formation of diverse nanostructures of metal oxides and sulfides with different morphologies when a laser with a long-pulse width (i.e., a millisecond pulsed laser) was applied, as shown in **Figure 3**.[36] Due to its lower power density (10^6–10^7 W cm^{-2}), the primary ablation products were mainly metal nanodroplets, which were ejected into the liquid medium at a high speed.[36] Due to their compactness, such hot metal nanodroplets were shown to react with the ambient medium gradually from the surfaces. The degree and rate of such reactions on the nanodroplet surface were primarily governed by the liquid reactivity and laser parameters, thus leading to products with different morphologies and chemical compositions.[36] Hence, the reactions and final products could be controlled by selecting appropriate liquids (and/or their concentration), targets, and laser parameters.[36–39]

Several groups also reported using a nanosecond pulsed laser to produce metal nanodroplets during LAL.[64,65] Tsuji et al. reported the formation of Ag, Au, and Si nanodroplets in water, which were investigated by means of a shadow graph. Straight jets of massive clusters and single droplets were observed along with bubbles of plasma on the target surface. The straight jets were suggested to be the main source of colloidal NPs, which formed in the jet via an aggregation and cooling processes.[21]

Phuoc et al. proposed another mechanism of metal nanodroplet formation.[66] They suggested that laser irradiation could cause a local melting of the metal target. Owing to the heat transfer from the metal target, the adjacent liquid layer was heated to a vapor or plasma state with a high pressure,[51,66] and the expanding vapor/plasma splashed the molten target into

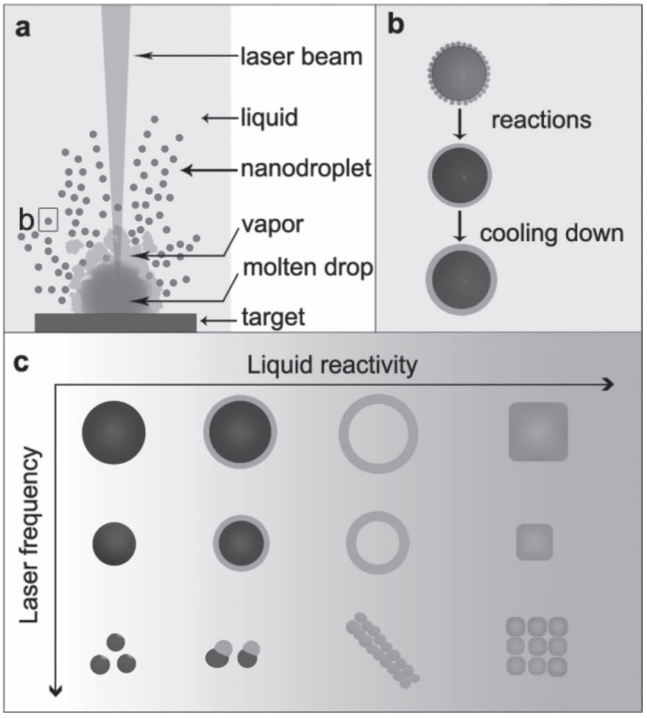

Figure 3. Schematic diagrams of metal nanodroplet ejection and nanostructure formation in the LAL process using a low-energy millisecond laser. a) Formation of nanodroplets. b) Reactions of an ejected metal nanodroplet with ambient liquid. c) Effect of liquid reactivity and laser frequency on the morphology of nanostructures formed when a Pb target was ablated in liquids. Reproduced with permission.[36] Copyright 2010, American Chemical Society.

nanodroplets, which then reacted with the liquid medium and produced the final nanostructures.[53]

In common LAL experiments, the thermal evaporation (i.e., vapor or plasma formation) and the explosive ejection of nanodroplets may occur simultaneously and thus their effects should normally overlap to produce nanostructures. Nichols et al. reported that the thermal evaporation generated fine Pt NPs with a uniform size, while the explosive ejection resulted in larger NPs with a wide size distribution and a significantly larger yield.[53–55] The multimodal character of size distribution was reported for various products prepared at different laser wavelengths and fluencies, suggesting that the two ablation mechanisms do coexist and manifest themselves in laser ablation processes and products.[36,54]

2.2. LAL Mechanism for Liquid Targets

In addition to the bulk target placed on the bottom of a liquid, various liquids can be adopted as a direct target, including suspensions with particles and solutions with precursors. For the former target, nano- and microparticles or powder/flakes could undergo a process of melting and vaporization or fragmentation, while the latter may experience photochemical or thermachemical reactions under laser irradiation.

2.2.1. Suspensions with Particles

Under laser ablation, particles in the suspension can transform into smaller sized particles of same or different shapes, phase, and composition.[67–75] Two mechanisms were proposed for the resizing and/or reshaping of the nanostructures and/or their surface modification using laser irradiation in liquid media. The first is the melting-evaporation mechanism, in which the laser induces melting and/or vaporization of larger sized particles into atoms or molecules, and then the produced atomic or molecular species rearrange into smaller nanostructures with the same or different shapes and crystal structures depending on the experimental conditions.[26–28,69,71] The second mechanism is the laser-induced Columbic explosion, which involves ejection of photoelectrons or thermal electrons from the surfaces of target nanostructures, leaving positive charges behind on the surface. The induced surface charges derive electrostatic repulsion between different parts of the primary particles, thus causing consequent fragmentation of a single particle into several smaller ones.[72–75]

The experimental conditions to switch on these two mechanisms are quite different. The former requires a high laser irradiance, which can make the temperature of the suspension particle target higher than its boiling point and thus vaporize the surface atoms and molecules. Meanwhile the latter requires a matching of the laser wavelength with the work function of the target material to eject photoelectrons. In picosecond or femtosecond laser systems, the laser intensity is high enough to allow multiphoton ionization to occur, which can induce fragmentation when the laser photon energy is even less than the work function. Recent theoretical investigations suggested that the fragmentation is the dominating process for femtosecond laser irradiation, while purely thermal evaporation occurs for nanosecond laser irradiation, even with an excitation wavelength of 355 nm.[67,68]

2.2.2. Solutions with Precursors

Laser irradiation of aqueous metal salts or liquid precursors is a bottom-up approach that can generate colloidal suspensions of NPs.[76–82] Metal salts are first photochemically induced to generate of neutral M^0 atoms, which then undergo clustering to form NPs. The neutral M^0 atoms can be obtained by either a direct photoreduction of metal ions using photochemically generated intermediates,[76–78] such as excited molecules and radicals,[79,80] or by using a photosensitive reagent that generates an intermediate via photoreduction. **Figure 4** illustrates a direct photoreduction and a photosensitized reduction mechanism for the photochemical synthesis of NPs.

Moreover, semiconductor NPs can serve as the substrate and reductant to produce metal/semiconductor nanocomposites.[83–85] When the NPs are excited by photons with energy higher than that of their bandgaps, electron and hole pairs are created. The produced electrons reduce metal ions adsorbed on the surface of the semiconductor NPs to produce M^0 atoms, which cluster to produce NPs or to form a shell layer on the surface of the semiconductor NPs resulting in semiconductor core/metal shell NPs. So far, many nanostructures, such as TiO_2/metal and ZnO/metal core/shell NPs have been successfully prepared based on this mechanism.[86–90]

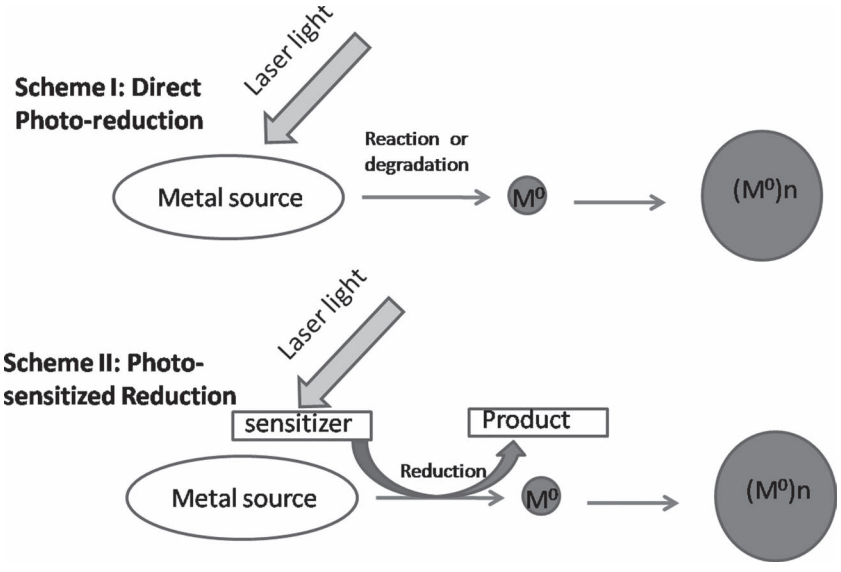

Figure 4. Schemes for direct photoreduction and photosensitized reduction of metal salt solution or liquid precursors (as metal source). Reproduced with permission.[81] Copyright 2009, Elsevier.

3. Various Methodologies Applied in LAL

3.1. Non-Reactive LAL

This method implies that there is no reaction between the ablated species and the surrounding liquid medium, and thus the formed nanostructures have the same composition as the applied targets. This is the most basic configuration for the LAL process that has been extensively exploited.[91–94] Silver, gold, and platinum metals have low reactivity with liquids and gases; therefore the PLA of these metals in most liquids is very likely to generate their corresponding elemental NPs.[24,45,91–94]

The LAL of a Ag target in electrolyte solutions (HCl, NaCl, NaOH, $AgNO_3$, and/or Na_2SO_3) using 1064 nm wavelength from a Nd:YAG laser has produced spherical Ag NPs with different surface morphologies.[91–93] The presence of HCl, NaCl, and/or NaOH during the PLA has led to the stabilization of the resulting Ag NPs, while the presence of $AgNO_3$ and $Na_2S_2O_3$ has shown a destabilizing effect.[91–93] Organic solvents (such as acetonitrile, *N,N*-dimethyl formamide, tetrahydrofuran, or dimethylsulfoxide) can influence the shape and structure of final products as well.[94] Moreover, the hydrodynamic diameter of Au NPs was demonstrated to decrease exponentially with the compressibility of water that depends on temperature.[45]

Mafune et al.[24] have studied the effect of anionic sodium dodecyl sulphate (SDS) concentrations, laser irradiance, and focussing conditions on the size, distribution, and abundance of Ag NPs produced by PLA of a Ag target in aqueous SDS. They have reported that the average size of NPs decreases, while size distribution first increases up to acritical miceller concentration (CMC), $\approx 8.1 \times 10^{-3}$ M, and then slightly decreases with an increase in SDS concentration. The average size of the NPs increases with the increase in laser pulse energy, while size distribution remains almost constant. **Figure 5** shows transmission electron microscopy (TEM) images and corresponding size histograms for NPs produced by LAL of a Ag target in aqueous of SDS with different concentrations.

The LAL of active metal targets (such as Zn, Cd, Cu, Ti, Al, Mg, Pb, and Fe) usually generates compound NPs through the reaction of a created plasma with the liquid. However, if the generation rate of the plasma species is high and the time for their clustering into particles is small, then the reaction between the plasma species inside the plasma dominates over the reaction between the plasma species and liquid medium

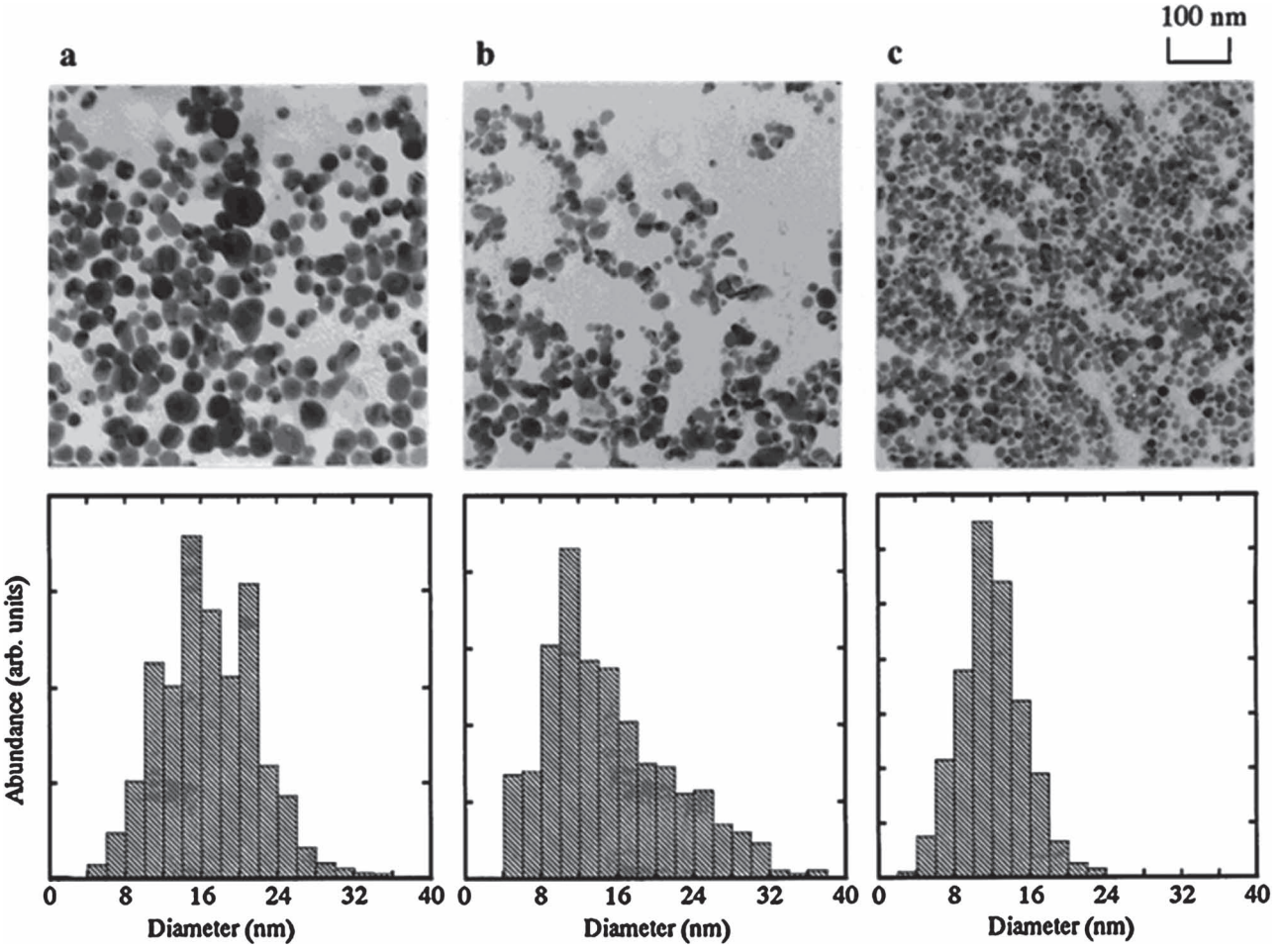

Figure 5. TEM images and corresponding size histograms of NPs produced by LAL of Ag target in a) 0.003 M, b) 0.01 M, and c) 0.05 M aqueous SDS.[45] Reproduced with permission.[45] Copyright 2011, American Chemical Society.

at the plasma/liquid interface. Under such conditions, active metal particles[95] or active metal core/metal compound shell particles[96,97] are produced. The LAL of active metals with stabilizing/capping agents also limits the reaction between the plasma species and liquid medium. There occurs a competition between the formation of pure metal clusters capped with surfactants and the reaction of plasma species with the liquid medium. For example, the LAL of Ti in ethanol and dichloroethane produced 35 nm cubic phase Ti nanocrystals,[98] and spherical Al NPs were produced by ablating an aluminum target in ethanol, acetone, and ethylene glycol.[99] Moreover, Co NPs in 0.003 mM ethylene glycol,[100] Ni NPs in water and 0.01 M aqueous SDS,[101] and tungsten[102] NPs in ethanol were also reported as typical examples of the non-reactive LAL of active metal targets.

3.2. Reactive LAL

Compared to the methods described in the previous section, this approach implies reactions between ablated species and liquid medium, and thus the formed nanostructures have a different composition from that of the targets. Obviously, this greatly expands the product composition spanning oxide, hydroxide, carbide, sulfide, nitride, and composite nanostructures that can be smartly designed via the reaction between selected targets and liquid media.

Laser induced plasma from a target material can heat the surrounding liquid medium turning it to plasma state, and the two plasmas can react fiercely to form metal compound nanostructures. The LAL of active metals in water or alcohols produces their hydroxides as the primary product.[96,103–113] These hydroxide seeds then either become dehydrated into oxide by losing water through hydrothermal reaction processes,[96,104] or become clustered to form hydroxide NPs.[112,113] The simultaneous flow of oxygen in the close vicinity of a laser produced plasma plume has the ability to modify the final products.[103,105,106] It increases oxygen content in the NPs, oxide/hydroxide ratio in nanocomposites, and the crystallinity of particles, while decreasing size and size distribution of NPs.[103] For example, the LAL of zinc in water or in alcohol produces zinc oxide[104] or $ZnO/Zn(OH)_2$ nanocomposites,[103] or ZnO/ZnOOH nanocomposite[105,106] particles. Similarly, the LAL of Ti in water produces TiO_x including TiO, TiO_2, and Ti_2O_3 NPs,[107–109] in liquid nitrogen, 2-propanol and n-hexane, it gives rise to TiN NPs,[110] TiO and TiC NPs,[98,111] and TiH[111] NPs, respectively. The LAL of Cd in water was reported to produce $Cd(OH)_2$ nanostructures.[112,113]

Golightly and Castleman[111] ablated Ti in 2-propanol, water, ethanol, and n-hexane and prepared TiC, TiO_x, and TiH NPs, respectively. LAL in water was reported to produce a larger amount of bigger (>70 nm) particles compared to those fabricated in 2-propanol, while the NPs prepared in n-hexane were smaller (<70 nm).[111] Irrespective of the liquid media used, smaller NPs were reported to incorporate more impurities.[111]

The surfactant concentration in the liquid media controls reaction rates at the plasma/liquid interface before the particle synthesis or at the particle/liquid interface after the production of NPs in the liquid, as well as the colloidal stability of the NPs.[96] With an increase in the surfactant concentration, the dominant reactions switch from those between the target plasma and liquid medium to those among the plasma species. As a result, the final product appears as pure metal compound NPs, core-shell NPs with metallic cores and metal compound shells, and metal NPs, successively.[96]

On the other hand, the effect of surfactant on the size and the shape of NPs and the stability of colloidal solution depend on the nature of charge on the NPs' surface and the nature of surfactant. For example, an increase in the concentration of SDS was shown to decrease both particle size and size distribution and to increase the colloidal stability of negatively surface-charged particles such as Zn or ZnO,[96] while it increased the size and rate of aggregation of positively surface-charged $Cd(OH)_2$NPs.[113] A layered $Zn(OH)_2$/DS nanocompositewas produced by the LAL of Zn in aqueous SDS,[114–116] and its morphology could be controlled through varying the composition of ethanol/water in liquid media.[117]

The reactive LAL of noble metals was also reported under such experimental conditions.[118–121] The LAL of Ag in 10^{-5}–0.1 M aqueous NaCl produced AgCl nanocubes.[118] Similarly, Ag_2O cubes, pyramids, triangular plates, pentagonal rods, and bars were obtained by the LAL of bulk Ag in polysorbate 80 aqueous solutions at room temperature.[119] Silver core/silver oxide shell NPs were produced by the femtosecond LAL of Ag in water and ethanol.[120] The LAL of Ag in aqueous KBr (0.1 M) as well as in a mixture of aqueous solutions of KBr (0.1 M) and aqueous SDS (0.01 M) produced AgBr NPs with irregular spherical shapes.[121]

3.3. Alloying and Fragmentation via LAL

As discussed in Section 2.2.1, if a suspension with particles is used as the ablating target, replacing the usually applied solid foils, some very interesting phenomena can be observed. The particles will undergo the process of melting/vaporization or fragmentation, giving rise to smaller sized particles of same or different shapes, phase, and chemical composition.

3.3.1. Laser-Induced Melting/Vaporization

Singh et al.[69] have produced α-Se quantum dots (QDs) via the laser irradiation of water suspended β-Se NPs with an average diameter of 69 nm. The size of the produced selenium QDs followed a second-order exponential decay function of irradiation time, finally reaching a minimum of ≈2.74 ± 2.32 nm.[69] **Figure 6** shows photographs and the variation in the size and bandgap energy of the α-Se QDs with irradiation time. Zeng et al.[70] applied the laser irradiation of a ZnO hollow sphere dispersion in water to produce ZnO QDs with sizes ranging from 1 to 8 nm. The following three stages of the process have been proposed by the authors: i) fragmentation of ZnO hollow spheres (0–10 min), ii) QD growth (10–20 min), and iii) ripening (20–30 min).[70]

Kawasaki has irradiated acetone suspended CuO powder using a 1064 nm nanosecond laser and reported the generation of ≈10 nm sized Cu NPs with a production rate of ≈1 mg min^{-1}.[112] The as-produced copper NPs then underwent a rapid aerobic

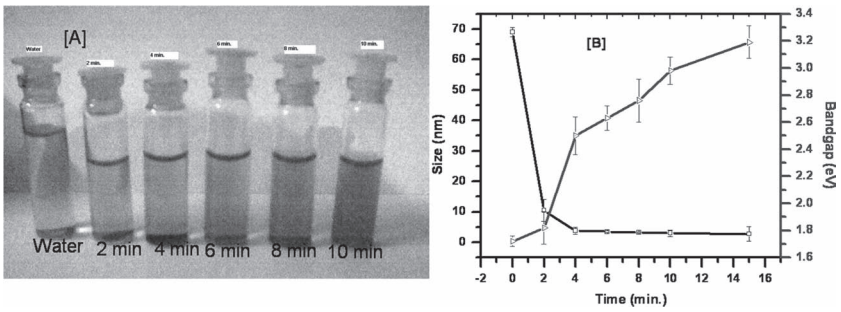

Figure 6. Suspension photographs, as well as the variation in the size and bandgap energy of the prepared α-Se QDs as they change with irradiation time. Reproduced with permission.[69] Copyright 2010, American Chemical Society.

oxidation process that converted them into Cu_2O particles. Similarly, Yeh et al. irradiated a 2-propanol suspended CuO powder by using either a 1064 nm or a 532 nm wavelength laser beam from a nanosecond Nd:YAG laser.[113] Mafune et al. have observed the formation of Au nanonetworks and small Au NPs through the 532 nm laser irradiation of ≈20 nm Au NPs.[71] The irradiation of water or low-content SDS solution suspended Au NPs led to a network formation where the size of the network increased with irradiation time, while the irradiation of particles suspended in a solution with higher SDS concentrations resulted in Au NPs with smaller sizes.[71]

3.3.2. Laser-Induced Columbic Explosion

Emission of electrons from a NPs' surface, through photoelectric effects, thermionic emission, and interaction with high kinetic energy particle beam, leaves the NPs charged positively. The generated positive charge on the particle surfaces may lead to the Columbic explosion of larger sized particles and the formation of smaller ones. Kamat et al.[72a] have irradiated water-suspended silver NPs using a picosecond pulsed laser operating at a 355 nm wavelength and 18 ps pulse width. They have observed that a biphotonic absorption process is responsible for the photoejection of electrons and the consequent Columbic explosion of the particles. Fujiwara et al.[72b] have reported the picosecond (18 ps, 532 nm) laser irradiation of water suspended thionicotinamide (TNA)-capped gold NPs. They have observed the formation of larger sized NPs during a short laser irradiation through the melting of aggregates, while smaller sized particles have been found as a result of a fragmentation at higher laser irradiance and/or a long term irradiation of particles. Giusti et al.[73] applied the irradiation of Au NPs with intense picosecond laser pulses (532 nm) and reported that a two-photon absorption process is responsible for the ejection of photoelectrons from the PAMAM G5 (fifth-generation ethylendiamine-core poly(amidoamine)) capped Au NPs and their consequent fragmentation into smaller sized NPs. Yamada et al.[74] and Muto et al.[75] used nanosecond laser irradiation of liquid-suspended Au NPs and reported the Columbic explosion occurring via the thermionic emission of electrons. The Au NPs were found to be thermally excited by the laser pulses, after which they were multiply ionized by the thermionic emission with positive charges on the surface, causing them to disintegrate through the Columbic explosion. A higher irradiance from the nanosecond beam was observed to cause higher surface charges and consequently quicker fragmentation.

3.3.3. Laser-Induced Alloying

The laser-induced photothermal melting or vaporization of metal NPs suspended in liquid media provides an efficient pathway for the synthesis of alloy NPs. The irradiation of a mixture of two (or more) colloids of elemental NPs can melt or vaporize them, thus making the formation of their alloys possible on condensation. Chen and Yeh[124] prepared Ag:Au alloy NPs with different compositions using the laser irradiation of a mixture of Ag and Au colloids mixed in different proportions. The surface plasmon resonance (SPR) absorption of such Ag:Au alloy NPs lies in between the SPR peaks of Au and Ag NPs with its position, λ_{max}, depending on the content of Au and Ag in the alloy. Zhang et al.[76] produced Ag:Au alloy NPs using 532 nm laser irradiation of a heterogeneous suspension of Ag (0.5–1 μm) and Au (0.8–1.5 μm) powders in aqueous 0.05 M SDS. The increase of Au content in the Ag:Au alloy NPs was demonstrated to causes a linear shift in the SPR absorption peak (λ_{max}) position towards longer wavelength. The color of the colloidal solutions of Ag:Au NPs and their UV-visible absorption spectra are presented in **Figure 7**.

3.4. Thermolysis via Laser Irradiation of Metal Salt Solutions and Liquid Precursors

The laser irradiation of metal salt solutions or liquid precursors is a bottom-up approach that generates a colloidal dispersion of NPs.[77–82,86] Here metal salts are photo-chemically induced to generate neutral M^0 atoms, which then undergo clustering to form NPs.[77–82,86] Photochemical synthesis is also a clean, quick, and simple process that provides i) a controlled synthesis of NPs and ii) a synthesis of NPs in various media such as sol, emulsion, glass, surfactant micelles, polymers, etc. Based on the processes involved, the photochemical decomposition of

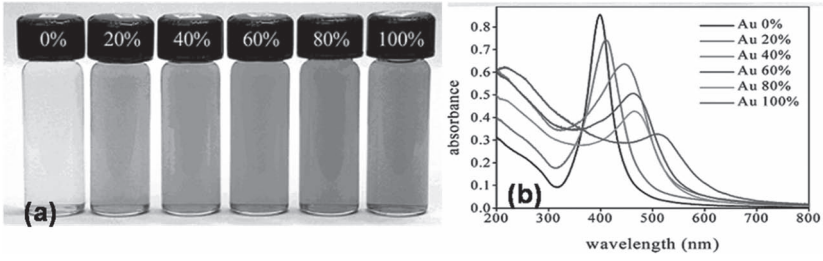

Figure 7. a) Photographs of colloid dispersions of Ag: Au alloy NPs of different compositions and b) corresponding UV-visible SPR absorption spectra. Reproduced with permission.[76] Copyright 2003, American Chemical Society.

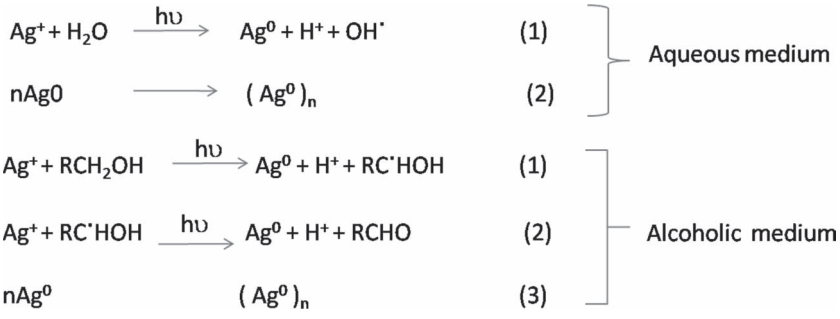

Scheme 1. Direct photoreduction of $AgClO_4$ in aqueous and alcoholic media for the sythesis of Ag NPs.[77] Copyright 1976, American Chemical Society.

metal salts or liquid precursors can be classified into two categories: photochemical synthesis and photocatalytic deposition.

3.4.1. Photochemical Synthesis

Photochemical synthesis is a bottom-up approach that involves photoreduction of ionic or molecular precursors to generate zero-valence metal (M^0) atoms under the conditions preventing their precipitation. The M^0 species are either produced by a direct photoreduction[77] of the source precursor. Alternatively, the reduction process is induced by photochemically generated intermediates such as excited molecules and radicals.

Scheme 1 shows direct photoreduction of $AgClO_4$ in aqueous and alcoholic media for the synthesis of Ag NPs.[77] In **Scheme 2**, dimethyl ketone serves as a photosensitizer for the reduction of M^+ ions into M^0 zero-valent atoms for the synthesis of $(M^0)_n$ NPs. Here an intermediate radical $(CH_3)_2C\cdot OH$ reduces metal ions into neutral atoms.[125–127]

3.4.2. Photocatalytic Deposition

The reduction of metal ions M^+ adsorbed on the surface of a semiconductor substrate has the ability to produce metal/semiconductor composites or semiconductor core/metal shell NPs.[84–86] Titanium dioxide is one of the best substrates for the photocatalytic decomposition of noble metal ions on its surface to prepare TiO_2 core/Au shell, TiO_2 core/Ag shell or TiO_2 core/Cu shell NPs.[87–89] A similar approach can be used for the synthesis of ZnO core/metal shell NPs.[90]

3.5. LAL with the Assistance of External Fields

LAL is known to produce plasma of target material and this hot plasma can, in turn, ionize a surrounding liquid medium into plasma state. The latter plasma may be called a plasma-induced plasma. Both plasmas contain electrons and ions, which can be driven by external electric and magnetic fields. Therefore, the application of external electric and magnetic fields to the plasma plume can control i) the kinetics of reactions at the plasma/liquid interface for the synthesis of product species, ii) the clustering of these product species into various nanostructures of controlled sizes and shapes, and iii) the assembly of these NPs into larger nanostructures. In addition, because the surfaces of NPs are charged, the application of electric field during ablation and/or after synthesis can affect their size, shape, and assembly.[43,128] The use of an external electric field also assists in the fabrication of high pressure nanophases, i.e., metastable phases of nanostructures that cannot be prepared under normal experimental conditions.[43,128]

Figure 8 shows an experimental setup for the electric field assisted laser ablation in liquid,[128] which includes a quartz chamber with a Ge target immersed into deionized water, a dc electric field produced by two parallel electrodes separated by 1.6 cm, and a 532 nm wavelength beam from a pulsed Nd:YAG laser. The magnitude of the electric field drives the size and shape of the produced nanostructures. For example, in the absence of an external electric field almost all prepared particles were pure Ge spheres with the size of 300 to 400 nm. The application of a 14.5 V dc voltage resulted in nano- and microcubes with sizes ranging from 200 to 400 nm, while a higher voltage of 32 V led to spindle-like GeO_2 nanostructures (**Figure 9**). The change in the composition of particles and valence of Ge with the application of electric field makes it possible to conclude that electric field helps in the laser-induced breakdown/decomposition of water molecules and generation of oxygen.[128] When a single crystalline Ge target biased with a dc voltage of –47 V was ablated in toluene, the LAL experiment generated single crystalline spherical Ge NPs with a metastable tetragonal phase along with residual cubic-phase Ge NPs.[43]

3.6. Gram-Scale Synthesis via LAL

Relatively low product yield is one of the main disadvantages associated with LAL. The simplest solution for scaling up

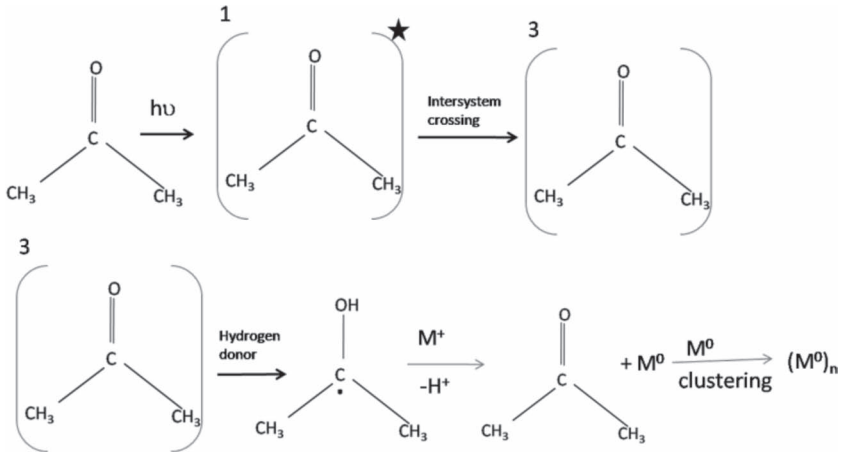

Scheme 2. Photosensitized reduction of the source precursor for the synthesis of metal NPs.[126] Copyright 2002, Royal Society of Chemistry.

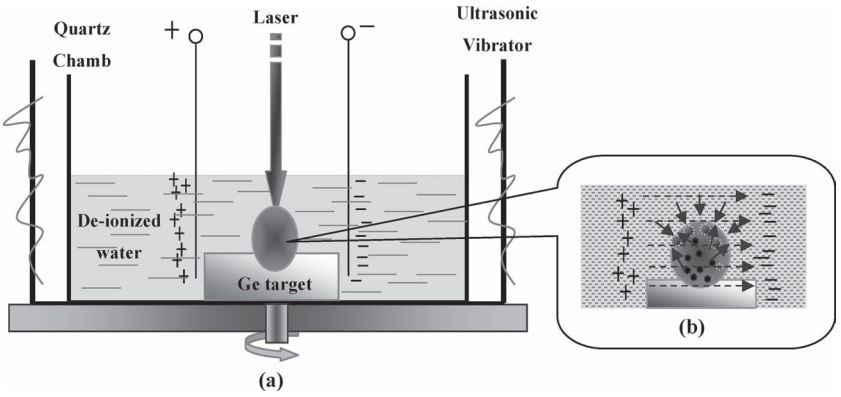

Figure 8. Experimental arrangement for electric-field-assisted pulsed laser ablation in liquid. Reproduced with permission.[128] Copyright 2008, American Chemical Society.

LAL-based synthesis is to optimize both laser (ablation time, laser irradiance, and repletion rate) and medium parameters (thickness of liquid above the target surface, liquid density, surface tension, and viscosity). However, there are more substantial factors determining the yield of product. The first one is the concentration of suspended NPs. In principle the number of produced NPs increases with ablation time, however as they absorb and scatter a portion of laser radiation, this reduces the number of photons at the target surface and lowers the ablation rate. The second factor is the cavitation bubble formed over the irradiated spot by the hot target, which in general has the same absorption and scattering effect as the suspended NPs. Especially at high repletion rates, e.g., 10 kHz, the life time of cavitation bubbles (>100 μs) is much longer than the interpulse separation time, and therefore the bubbles can remarkably affect the laser pulse. The third factor is the heat-and-shock-wave-affected zone generated by the laser pulse, which can facilitate the interaction of the next laser pulse with the target. Usually such a zone is even larger than that covered by the cavitation bubble.[129,130]

Liquid circulation above the target surface can remove NPs and cavitation bubbles from the ablation zone. On the other hand, the scanning optics technique can help the laser beam cross the spatial (50–200 μm) and temporal (100 μs) dimensions of cavitation bubbles when a properly adjusted scanning speed is used. This can help position the next laser pulse beyond the cavitation bubble generated by a current pulse but within its heat-and-shock-wave-affected zone, as shown in **Figure 10**b, and achieve higher ablation rates and product yield on the order of grams per hour (Figure 10a).[129] Both of the above techniques permit one to attain higher productivities, up to gram-scale yields of NPs by using LAL.[129,130]

4. Various Nanostructures Fabricated via LAL

4.1. Metal, Oxide, and Hydroxide Nanoparticles

Typically, the most common products prepared via the LAL method are metal NPs or NPs of metal compounds formed via the reaction of ablated metal with liquid media. In a typical LAL setup, a metal target is normally immersed in a liquid medium and then the laser is focused on the target through the transparent liquid.[131] When the target is a noble metal or material such as carbon or silicon, the ablated products are usually pure elemental particles,[132] which are formed in the laser generated plasma in the absence of any chemical reactions with the liquid medium. This is especially so when surfactants are added, thus stabilizing the produced NPs as a dispersion in the liquid.[91,133,134] On the contrary, when more active metals are used as the target, the as-prepared metal NPs are normally reported to react with water (present in the liquid media), leading to the formation of oxide or hydroxide nanostructures.[37,39,135,136]

In addition to metal targets, some reactive liquid media can also act as targets to absorb laser beam energy and produce compound NPs. As an example, Henley and co-workers took advantage of laser heating along with the traditional hydrothermal

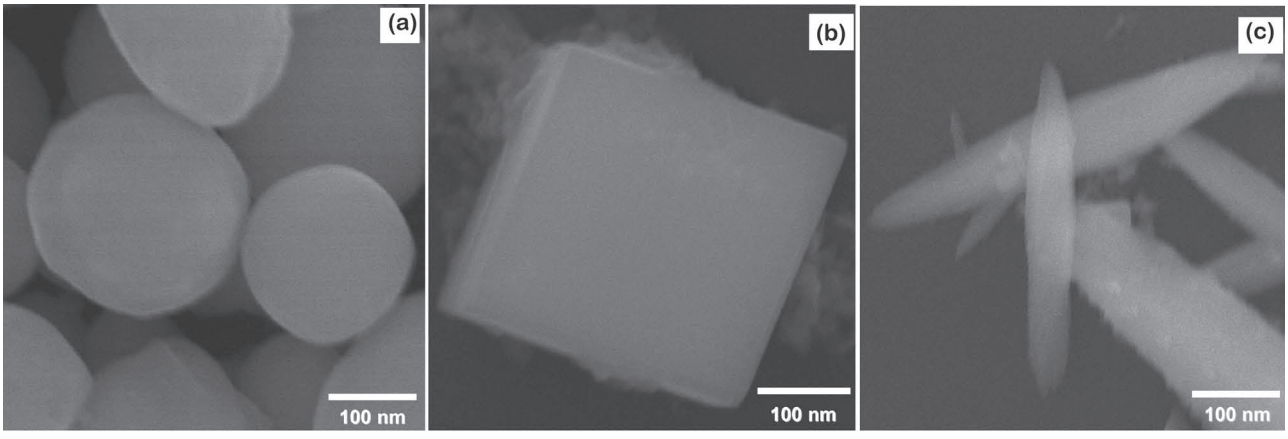

Figure 9. SEM images of nanostructures produced by a) conventional LAL and b,c) electric-field assisted LAL with b) 14.5 V and c) 32 V dc voltages. Reproduced with permission.[128] Copyright 2008, American Chemical Society.

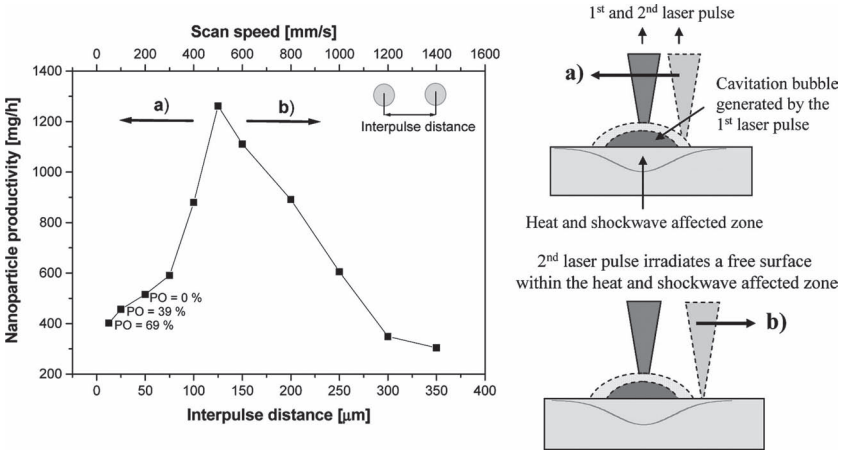

Figure 10. Variation in the productivity of NPs with interpulse distance and scan speed employing laser pulse energy of 4.6 mJ per pulse, 4 kHz repetition rate, and 4 mm thickness of the liquid layer. Schemes of ablation, laser pulse, cavitation bubble, and heat-and-shock-wave-affected zone. Reproduced with permission.[129] Copyright 2010, American Chemical Society.

synthesis, employing a 248 nm KrF excimer laser to irradiate precursor solutions for the synthesis of ZnO nanocrystals.[137] In another study, a CO_2 laser was used to heat water/alcohol solutions saturated with $Zn(AcAc)_2$, which led to the decomposition of the precursor and fabrication of ZnO nanorods.[138] When an excimer laser (248 and 308 nm) or a continuous wave (cw) Ar^+ laser (488 nm) were employed to irradiate solutions containing certain metal salts, the laser-induced decomposition of precursors could lead to the formation of pure metal (Pd, Cu, and Ag) particles in the solutions.[139] Thus, the laser-induced liquid phase decomposition has become an efficient technique for the synthesis of metal or oxide NPs.[140]

4.2. Nanoparticles of Unique Phases

One of the most unique features of the LAL technique is the extreme local conditions generated by the laser inside the ablation-induced plasma and at its boundary with the liquid medium. The plasma phase is very hot and composed of highly excited species possessing high temperature, high pressure and high density (HTHPHD). Neighboring and surrounding the plasma, the liquid phase leads to its rapid quenching.[141] This interaction between the plasma and liquid phases may therefore result in the appearance of unusual phases as products quenched extremely quickly from very high temperatures.

As an example, metastable zinc peroxide (ZnO_2) NPs could be produced by ablating a metal zinc target in 3% H_2O_2.[40] Liu et al. ablated a Si target in a solution of certain inorganic salts, which facilitated the formation of Si microcubes with a zinc-blende structure.[41] By applying the same approach and using single-crystal Si substrates covered with ≈150 to 300 nm thick amorphous carbon as targets, the same group obtained a novel type of carbon micro- and nanocubes with a C8-like structure.[42] A high-pressure phase, the tetragonal structure of Ge, was reported to be trapped in the form of nanocrystals via the electrical-field assisted LAL at ambient pressure and temperature.[43] Silicon nanocrystals with atypical face-centered cubic (fcc) crystal structure were synthesized through a long-pulse (microsecond) laser ablation in water.[142] The long pulse width of the adopted laser was shown to be favorable for the generation of high-temperature, high-pressure conditions, which were responsible for the formation of such fcc Si nanocrystals.[142]

By laser-ablating a Ti target, TiO_2 nanospheres with a mixed-phase (rutile/anatase) structure were fabricated by Tian et al.,[143] who also concluded that rapidly changing temperature and pressure were responsible for the coexistence of the rutile and anatase phases in the product.[143] While preparing nanodiamond crystals via the pulsed-laser irradiation of a graphite powder in water, Hu et al.[144] found that single-crystal nanodiamond particles successively grew into uncommon, multiply-twinned structures through intermediate simple-twin and triple-twin structures.[144]

The above results prove that the LAL process can produce nanostructures with uncommon and atypical phases, which are only stable at high temperatures and high pressures and are metastable under normal conditions. On the other hand, the high temperature, high pressure and high density conditions generated during the LAL can change the formation dynamics of various (mainly surface) defects and thus lead to NPs with unique defect states. The rapid quenching is very likely to preserve such unique defects formed under extreme conditions, thus also contributing to the preparation of various unique nanostructures.

4.3. Nanostructures with More Complex Morphology

Besides a range of metal or metal compound NPs, the LAL approach has also been applied to fabricate many nanostructures with other, more complex, morphologies. For 0D nanostructures, such as hollow and core/shell nanostructures and nanocomposites, Niu et al. adopted a long pulse-width (millisecond-scale) laser to ablate a number of metal targets in liquid media with different chemistry and reactivity.[36,39] The low-power density of the applied millisecond laser was found to be favorable for the generation of metal nanodroplets, which in turn reacted with the liquid medium giving rise to diverse nanostructures, such as hollow NPs, core/shell NPs, heterostructures, nanocubes, and ordered arrays of several metal oxides and sulfides (see **Figure 11**).[36,39] Composite Au/TiO_2 NPs were reported to be prepared by laser ablating an Au plate in a TiO_2 sol,[145] and similar composite NPs of Au and SnO_2 could also be synthesized by nanosoldering of pure Au and SnO_2 NPs.[146] In the latter work, Au and SnO_2 colloids were first produced via laser ablation and then mixed and soldered by further laser processing to form nanocomposites.[146]

Jimenez et al.[147] designed smart reaction systems to produce composite NPs via the laser ablation of reactive targets immersed in water solutions of metal salts. As an example,

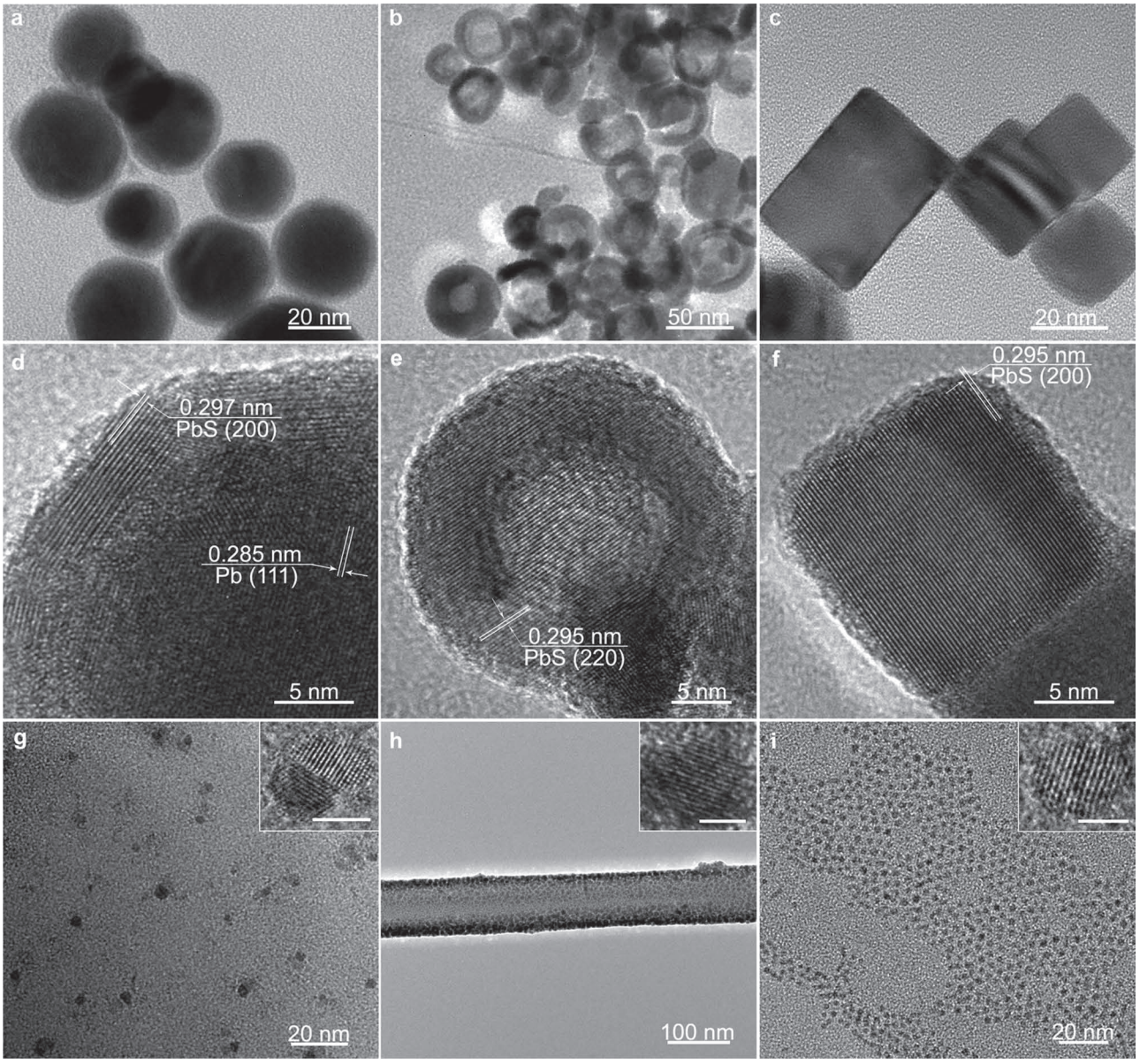

Figure 11. TEM images of various nanostructures obtained via LAL by ablating Pb in various S-containing liquids and using different laser parameters: a) core/shell NPs with Pb core and PbS shell; b) PbS hollow NPs; c) PbS nanocubes; d–f) high-resolution TEM (HRTEM) images of the nanostructures in (a–c), respectively; g) Pb-PbS heteronanostructures; the inset shows a HRTEM image of a Pb-PbS NP; the scale bar indicates 3 nm; h) a PbS polycrystalline nanotube; the inset shows a HRTEM image of a NP in the nanotube; scale bar indicates 3 nm; and i) ordered arrays of PbS nanocrystals; the inset is a HRTEM image of such a nanocrystal; scale bar indicates 3 nm. Reproduced with permission.[36] Copyright 2010, American Chemical Society.

when a Si target was ablated in an aqueous solution of $AgNO_3$, the generated Si NPs then reacted with $AgNO_3$ and water to produce Ag/SiO_2 core/shell nanostructures with Ag cores and SiO_2 shells via the following reaction: $Si(NP) + 4AgNO_3 + 2H_2O \rightarrow SiO_2(NP) + 4Ag(NP) + 4H^+ + 4NO^-_3$

Similarly, $(Au, Ag)/SiO_2$ core/shell nanostructures could also be obtained. Such nanostructures are presented in **Figure 12**, with a schematic model of a particle shown in panel (f).[147]

When a Si target was ablated by Shirahata et al. in an inert organic liquid, e.g., 1-octene, the as-produced Si NPs were found to be terminated with organic monolayers through covalent C–Si bonds.[148] Similarly, when carbon black or graphite powders were irradiated by a pulsed laser in organic media (diamine hydrate, diethanolamine, and poly(ethylene glycol)), luminescent carbon NPs could be obtained with carboxylate ligands on their surface.[149] In another study, carbon-encapsulated magnetic NPs were synthesized by irradiating a solution containing various metallocenes with a nanosecond pulsed ultraviolet laser. The products showed diameters ranging from a few nanometers to about 300 nm.[150]

As for 1D nanostructures, Singh and Gopal reported the synthesis of a variety of Cd hydroxide nanostructures from NPs

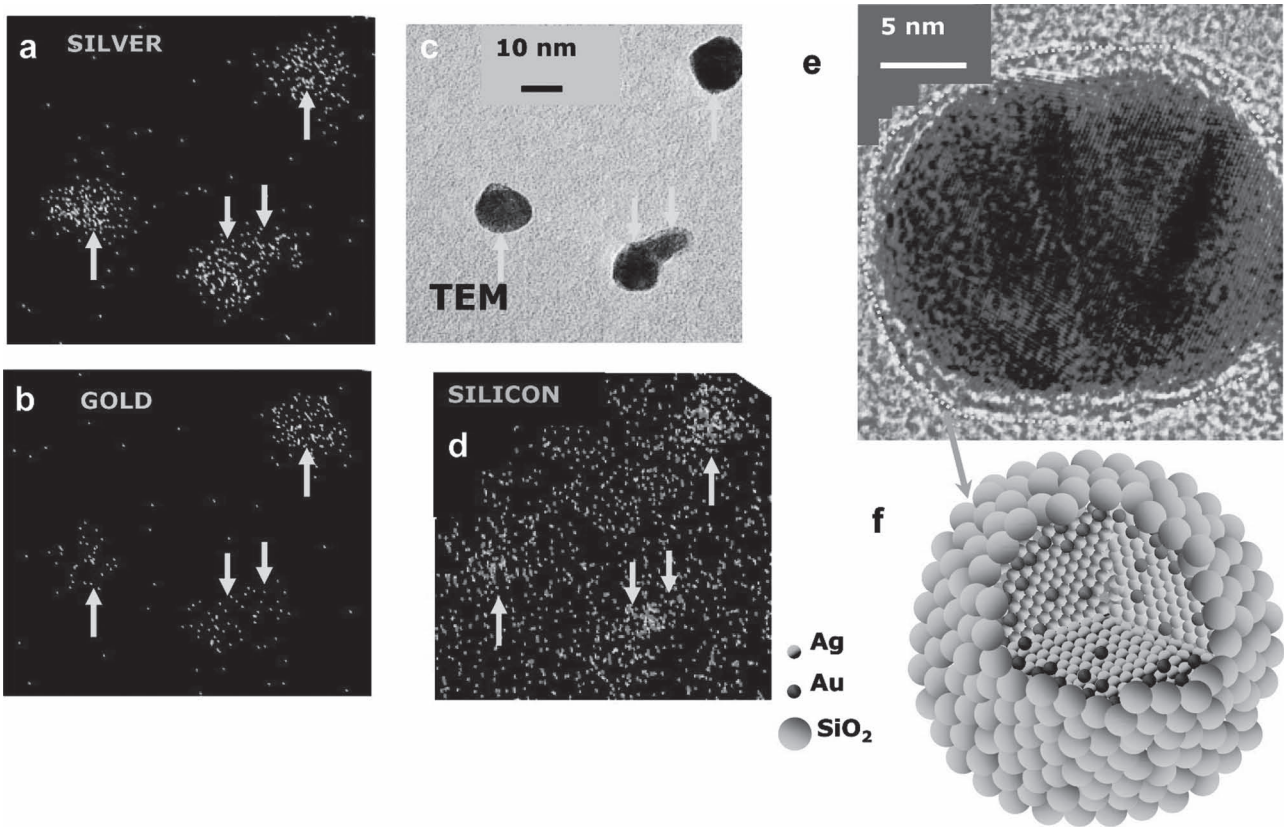

Figure 12. Energy dispersive X-ray high-resolution TEM (EDX-HRTEM) chemical mapping images of Ag-Au alloy NPs demonstrating the presence of a) Ag and(b) Au in four NPs marked by yellow arrows and observed in c) as a TEM image. d) Apart from Ag and Au, the EDX-HRTEM also reveals the presence of Si which is mainly concentrated around the NPs. e) A HRTEM image and f) a schematic model of a NP, where a yellow dotted line in (e) indicates the limit of SiO_2 shell. Reproduced with permission.[147] Copyright 2010, American Chemical Society.

to nanorods, nanotetrapods, nanoflower buds, and 2D and 3D nanoflowers.[113] The experimental procedure consisted of the nanosecond pulsed laser ablation of a Cd rod placed on the bottom of a glass vessel with aqueous SDS with different concentrations. The initially produced spherical NPs were observed to self-assemble into 1D nanorods and then to more complex nanoarchitectures based on them.[113] Similarly, ZnO nanocrystals with controllable morphologies were synthesized by Jayawardena et al. via a hybrid growth approach by combining laser heating with a traditional hydrothermal synthesis.[137] In their work, a laser induced photothermal breakdown effect was found to compete with the Ostwald ripening, determining the morphology of final products.[137] More specifically, ZnO NPs formed via the photothermal breakdown at the highest laser power fluence acted as the seed for further ZnO growth, leading to the formation of bi-, tri-, or tetrapod-like structures.[137]

Singh and Gopal[104] used the LAL of zinc in methanol and reported the synthesis of drop-shaped zinc oxide QDs and their self-assembly into various dendritic nanostructures. The dendritic assemblies were classified into the following three categories: i) linear axis symmetrical branching, ii) linear axis asymmetrical branching, and iii) curvilinear axis asymmetrical branching. **Figure 13** presents the assemblies of such drop-shaped zinc oxide particles into various dendritic nanostructures and schemes for their branching with axis.

In another study, a fast and large-scale approach for the synthesis of iron oxide nanowires at room temperature was described in which pulsed-laser (248 nm) ablation of iron powder in methanol was exploited.[151] Furthermore, by applying electrical-field-assisted LAL, Lin et al. reported the synthesis of CuO nanocrystals with their subsequent assembly occurring within one step.[152] As a result, a functional CuO nanostructure with a complex shape (nanospindles) and shape-dependent optical absorption was prepared.[152]

For 2D products, layered AgBr based inorganic/organic nanocomposites were prepared via the LAL of a Ag target in the aqueous media of cetyltriethylammonium bromide (CTAB), tetradecyltrimethylammonium bromide (TTAB), and sodium triacetoxyborohydride (STAB).[121] The obtained AgBr nanostructures had 2D shapes and the size of nanosheets could be changed with the surfactant concentration. The nanocomposites were composed of alternating organic and inorganic lattices in which cationic surfactant molecules were adsorbed between the anionic AgBr interlayers with an interdigitated bilayer arrangement.[121]

As a summary, the pulsed LAL shows potential as a relatively simple, versatile, and promising technique for the synthesis of diverse nanostructures with different chemistries and morphologies, including NPs, hollow NPs, core/shell NPs, heterostructures, nanocubes, ordered arrays of NPs, 1D nanorods,

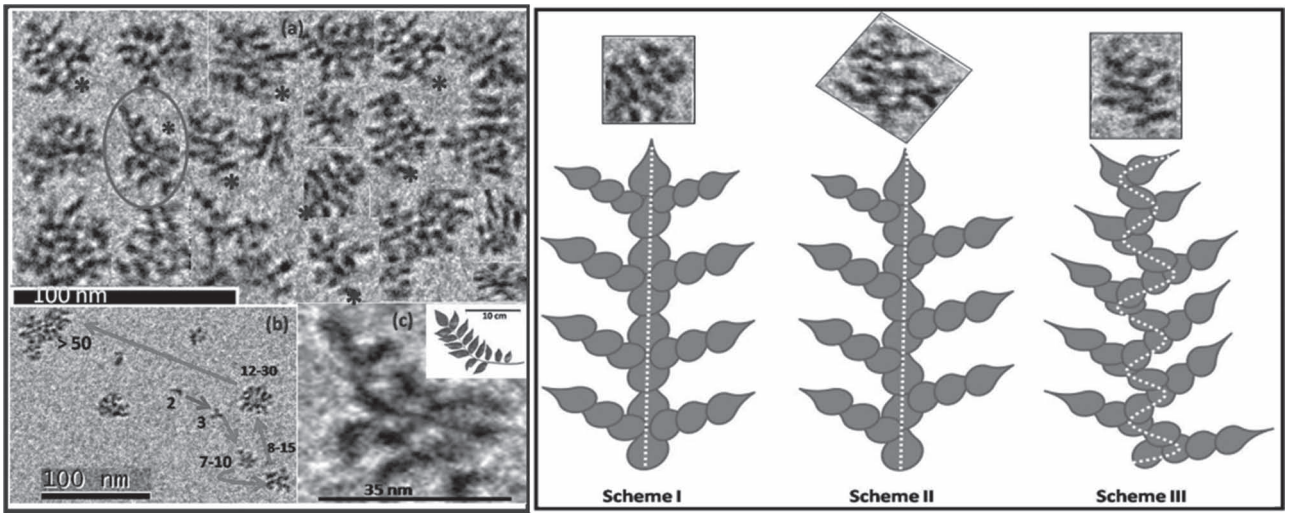

Figure 13. Assemblies of drop-shaped zinc oxide QDs into various dendritic nanostructures and three possible branching schemes. Reproduced with permission.[104] Copyright 2011, Elsevier.

and their successor nanoarchitectures. This certainly exceeds common expectations based on the "typical" products of this technique (i.e., metal, C, Si, and compound NPs), which have been long prepared by conventional laser-ablation methods.

5. Applications of LAL-Formed Nanomaterials

5.1. One-Step, Functionalized Noble Metal NPs for Bioapplications

Bioconjugated NPs have attracted increasingly more attention as convenient and important analytical tools for biological and medical applications. If certain surfactants, polymers, or biomolecules are added into the liquid medium, the in situ conjugation onto the NP surfaces can be realized, as shown in **Figure 14**.[44–46,161] In situ functionalization during the LAL formation of NPs was first envisaged to improve the stability of obtained colloids,[153] while currently it aims at the one-step preparation of bioconjugated NPs.[44]

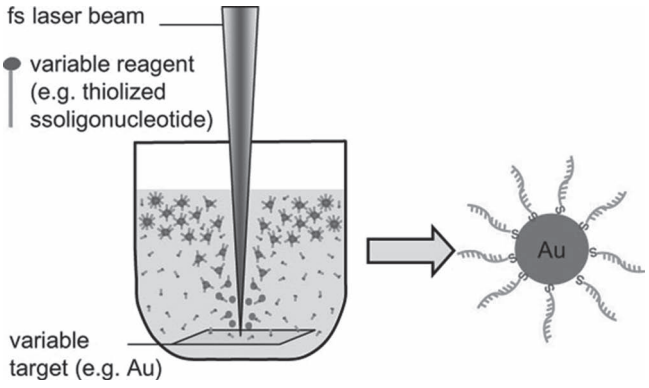

Figure 14. Schematic illustration of the in situ bioconjugation process for NPs via laser ablation in liquid. Reproduced with permission.[44]

This approach has been widely adopted for the synthesis of gold, silver, and copper NPs in situ functionalized with amphiphilic copolymers[44,47] and organic monolayer-covered Si nanocrystals.[148] For instance, Salmaso et al. prepared Au NPs with thermoresponsive thiol terminated poly-*N*-isopropylacrylamide-*co*-acrylamide copolymer.[154] Cell culture studies showed that the polymer decorated Au NPs could be located into human breast adenocarcinoma MCF7 cells treated at 40 °C (12 000 Au NP per cell) with an up-take more than 80-fold greater compared to cells treated at 34 °C with the same particles (140 Au NP per cell). Moreover, Walter et al. applied LAL-formed aptamer-conjugated Au NPs in solid-phase assays.[155] As shown in **Figure 15**, Au NPs conjugated with anti-prostate-specific membrane antigen (anti-PSMA) aptamer exhibited a staining pattern similar to anti-PSMA antibody. In both cases, a positive staining of acinar epithelial cells was observed. In tissue sections treated with anti-PSMA aptamer-conjugated Au NPs, an additional staining of muscle cells was observed that was not detected in the positive control. This result demonstrates that the anti-PSMA aptamer Au NPs conjugates can detect PSMA in acinar epithelial cells of human prostate cancer.

5.2. Semiconductor NPs for Luminescence Applications

LAL has been widely applied for the fabrication of luminescent semiconductor NPs, which have attracted much attention due to their broad-range of important applicatons.[70,96,156–165] Because of the non-equilibrium thermodynamic features of the technique (transient plasma process with high temperatures, high pressures, ultrafast chemical reactions, and high rate thermal quenching), high-density defects, uncommon microstructures, and metastable phases have been often reported for LAL-generated NPs.[49] That is why semiconductor NPs, such as ZnO, Si, SiC, and W_2C, prepared by this technique have been reported to exhibit unique photoluminescence properties that are different from those observed from NPs fabricated via conventional methods.[48,60,157,164–166]

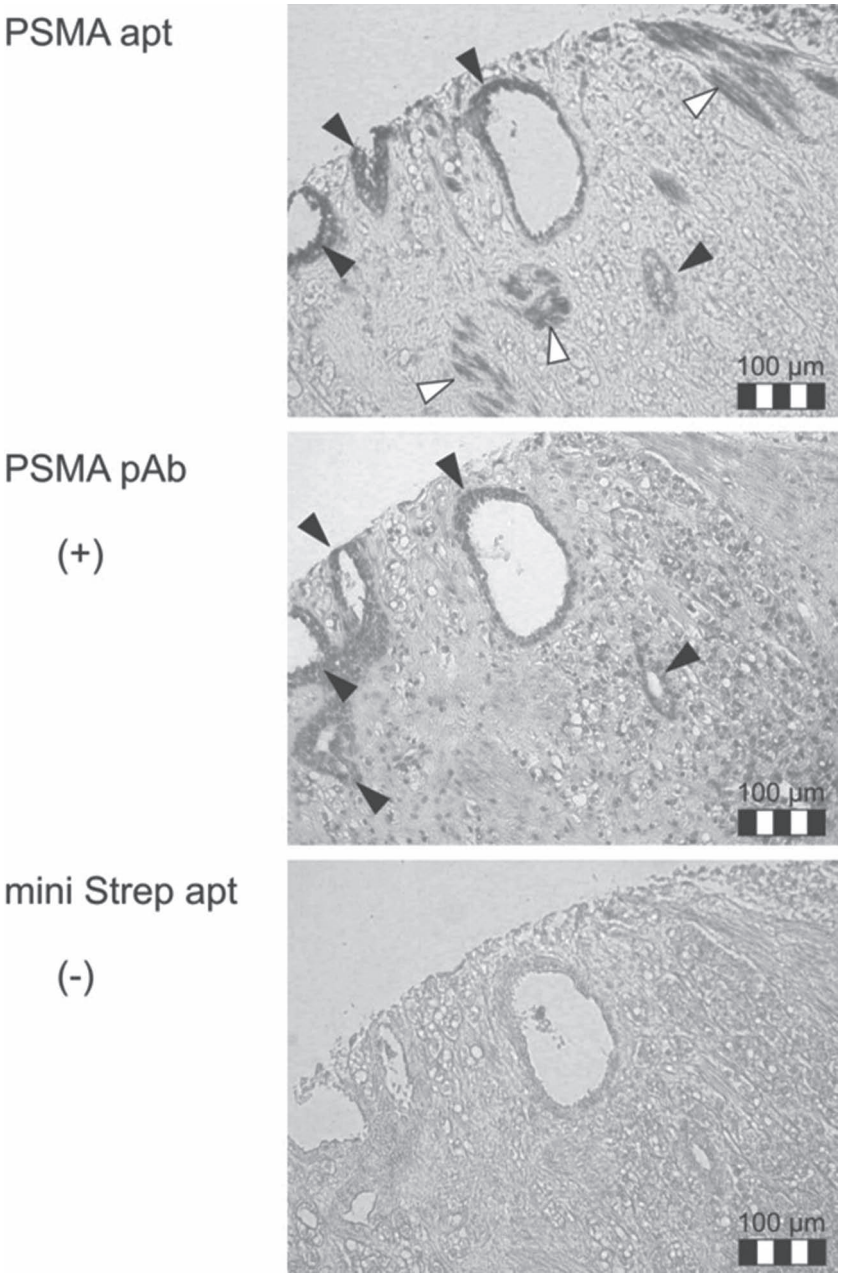

Figure 15. Detection of PSMA positive structures in prostate cancer tissuesections by immunohistochemical staining using anti-PSMA aptamer (PSMA apt)-conjugated Au NPs. As a negative control, Au NPs conjugated with miniStrep aptamer (miniStrep apt) were used. Apolyclonal antibody directed against PSMA (PSMA pAb) was used as a positive control. The positive control was additionally stained with aematoxylin and Eosin. Black arrows indicate specific staining, while white arrows show unspecific binding. Reproduced with permission. [155] Copyright 2010, Springer.

Figure 16a shows the photoluminescence (PL) spectra of Zn/ZnO core/shell NPs with different shell thicknesses and microstructures prepared by using LAL.[48,158] All the samples exhibit a strong violet emission peak centered at 425 nm (2.92 eV) with a vague band tail in the green range. The intensity of violet emission is seen to increase with the decrease in shell thickness (decrease of applied laser power). Furthermore, the visible emission of the Zn/ZnO NPs could be shifted from 440 to 555 nm through low-temperature annealing, as shown in Figure 16b.[49,50,70] Although visible emission is universally considered to be associated with intrinsic or extrinsic defects in ZnO-based materials, there are still numerous controversies on their defect centers and unambiguous electron transitions. The most typical visible emission of ZnO appears as a green band. The ZnO emission in the violet-blue spectral range, shown in Figure 16a, is very rare, indicating the existence of unusual defect states due to the unique features of LAL as a preparation approach. The violet-blue light emission demonstrated by the LAL-generated Zn/ZnO NPs and the possibility to tune their emission properties within a large spectral range make such materials very beneficial for applications in light emitters, display devices, and biological labeling.[49,162–174]

Alternatively, LAL could be used to fabricate doped and complex oxide NPs due to the strong ablating ability of laser beam. Ledoux and co-workers prepared highly luminescent NPs of Y_2O_3:Eu, Lu_2O_2S:Eu, Gd_2SiO_5:Ce, Lu_3TaO_7:Gd, Lu_3TaO_7:Tb, Y_2SiO_5:Ce, $GdTaO_4$:Tb, and $Gd_{0.4}Y_{2.6}Al_5O_{12}$:Ce using LAL.[165] Their results demonstrated that LAL can be used as a fast method to prepare complex nanosized materials with luminescent properties in four different material families: sesquioxydes, oxysulfides, silicates, and tantalates. The size distribution of the products was monodispersed and characterized by mean sizes of roughly 7 nm.[165,166] The last point is of particular interest because NPs within this size range are large enough to preserve the luminescent properties of the bulk material and yet small enough for applications such as biolabelling or anticounterfeit marking.[167]

5.3. NP Thin Films for SERS Detection Applications

Trace chemical and biomolecule detection is of particular importance in environmental pollution monitoring, anti-drug smuggling, anti-terrorism, and biorelated fields. Surface enhanced Raman scattering (SERS) has rapidly grown as a powerful tool for the above applications because of its high selectivity and sensitivity. In this context, because of their more pure surfaces, noble metal NPs prepared by LAL were demonstrated to perform better as components of SERS active substrate, when compared with their chemically obtained counterparts.[27]

Prochazka and co-workers fabricated Ag NPs via the laser ablation of Ag foil in water and explored their SERS

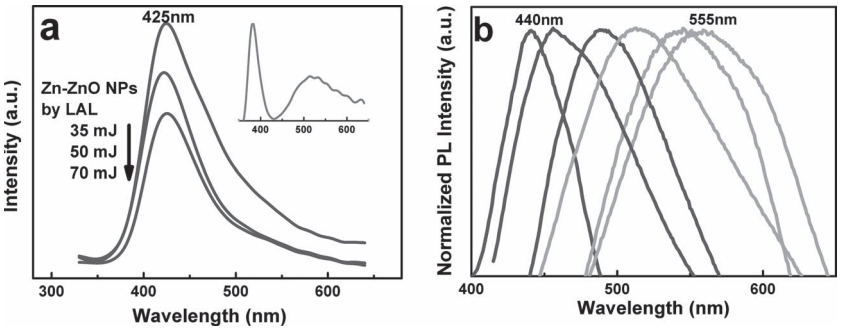

Figure 16. a) Violet-blue photoluminescence spectra of Zn/ZnO core/shell NPs obtained by LAL with different laser powers. The inset presents the usual UV and green emission of ZnO NPs after high-temperature annealing. b) Normalized visible emission spectra from blue to green regions recorded for ZnO NPs fabricated by LAL and treated under different low-temperature annealing conditions. Reproduced with permission.[49]

performance.[168] Compared to chemically produced Ag NPs, those prepared by means of LAL were reported to demonstrate a better reproducibility of SERS signals. The kinetics of metalation of the free base 5,10,15,20-tetrakis(1-methyl-4-pyridyl) porphyrin (H_2TMPyP) adsorbed on the Ag colloids was used as a comparative test of the reproducibility of the SERS spectral information, as shown in **Figure 17**. The metalation process was faster for the laser-ablated NPs than for the chemically prepared ones, since the residual anions, which slow down the metalation of H_2TMPyP, were not present on the surfaces of the former NPs. An excellent reproducibility of the porphyrin metalation rate was repeatedly observed for the same ablated colloids after one day, one month, and even ten months of aging. In contrast, significant variations of the metalation rate were observed for the borohydride-reduced Ag colloids over several days of aging.[168]

In addition to the reproducibility, the structural uniformity of the SERS substrate is also very important for its practical application. Recently, Yang et al. assembled LAL-formed Ag colloids to form SERS active substrates via electrophoretic deposition onto a colloidal crystal template.[92,169] The film surface roughness and the distance between the Ag NPs could be controlled

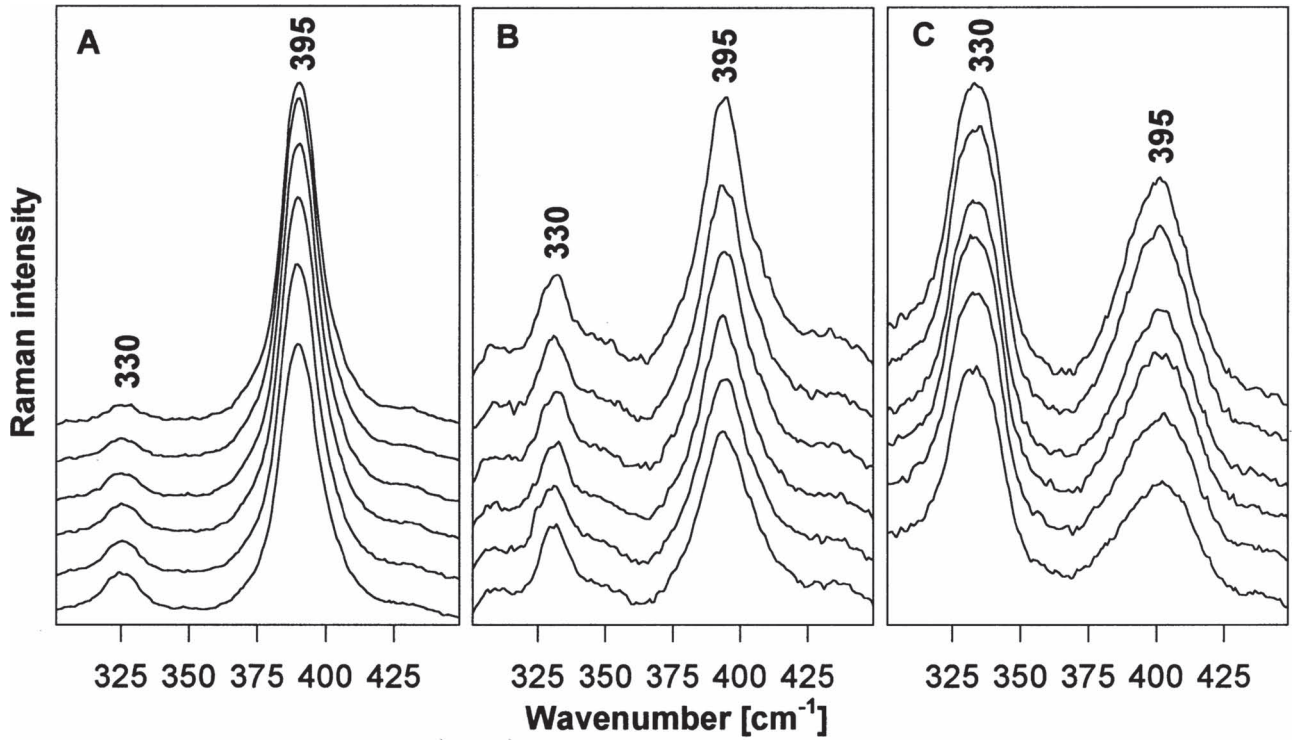

Figure 17. Time evolution of the free base (330 cm^{-1}) and the Ag metalloporphyrin (395 cm^{-1}) marker bands in the SERS spectra of Ag colloid/H_2TMPyP system: a) ablated, b) borohydride-reduced, and c) citrate-reduced Ag colloids. SERS spectra were measured on the time scale of 40 s to 20 min; bottom spectra were obtained 40 s and top spectrum 20 min after the preparation of the system. Reproduced with permission.[168] Copyright 1997, American Chemical Society.

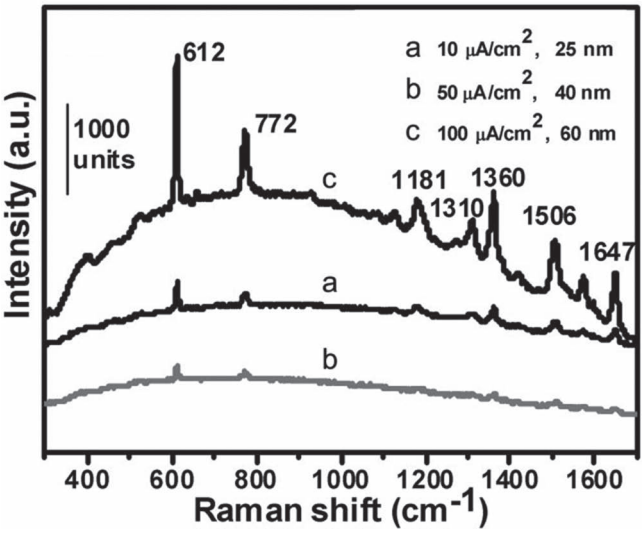

Figure 18. SERS spectra of Rodamine 6G (R6G) molecules adsorbed on Ag nanoshells, which were composed of LAL-formed NPs with different sizes. All SERS data are averaged over 5 scans on randomly chosen areas and the standard deviation was less than 10%. Reproduced with permission.[169]

by the deposition current density and plasma etching time. The Ag nanoshells composed of Ag NPs with the size of 60 nm were found to exhibit both strong SERS enhancement factors and excellent SERS signal reproducibility, as shown in **Figure 18**. The results demonstrated that both size and interdistance tuning of NPs could be used for the optimization of SERS performance. Furthermore, the LAL technique is well known for its ability to prepare alloyed metal particles, e.g., AuAg NPs.[170,171] The oxidation resistance of alloyed NPs is known to be composition dependent, which can be used to enhance significantly the performance (durability and stability) of SERS substrates.

5.4. Nanofertilizers for Seed Germination and Growth Stimulation

The use of nanomaterials in the area of plant science is relatively young, but it is quickly emerging with the expectation that the small-sized particles might increase the productivity of crops to fulfill the future demands of progressively growing populations in Asian region, as well as provide more fresh produce for other regions. Nanoscale materials were also reported to stimulate the increase of oxygen evolution capacity of plants, which is attractive for a better biosphere. Singh et al.[172] tested PLA synthesized anatase TiO_2 NPs as nanofertilizers for the stimulation of seed germination and plant growth of *Brassica oleracea* as shown in **Figure 19**. It was observed that certain concentrations of the colloidal TiO_2 NPs stimulate the seed germination and growth of the *Brassica oleracea* plant.[172] Various physical parameters of the plants (such as radical length in the germinated seeds, the number of leaves, leaf area, height, etc.), as well as the amount of chlorophyll a, chlorophyll b, and carotenoid were found to increase with the increase in NP concentration, attain their maximum values near 1.5 mM and then start decreasing at higher (>2.0 mM) concentrations.[172] It was concluded that lower amounts (<2.5 mM) of the NPs is beneficial for the growth, germination, various biochemical parameters, and overall health of the *Brassica oleracea* plants.[172] The high colloidal stability of laser-synthesized anatase TiO_2 NPs facilitated their dispersity and availability in the plant growth media for longer time.[172]

5.5. Other Applications

In addition to the above-mentioned applications, various LAL-generated nanostructures can also be used in catalysis, as various energy-related materials, in photothermal therapy fields, etc. Taking advantage of the non-equilibrium nature of the LAL technique, Liu and co-workers prepared TiO_2 NPs with the rutile phase, which is the most thermodynamically stable phase, but difficult to obtain via conventional low-temperature approaches.[171] Experiments involving the degradation of methylene blue demonstrated that such LAL-formed rutile TiO_2 NPs had a very high photocatalytic activity.[171] Excellent photocatalytic properties were also exhibited by LAL-prepared $(La,Sr)CoO_3$ NPs deposited on ZnO nanorod arrays.[173] Zeng et al. developed a selective etching method to convert common LAL-prepared core/shell NPs into hollow oxide NPs and noble metal-oxide composite NPs, such as Au/ZnO, Pt/ZnO, and Au/Pt/ZnO NPs.[173,174] These nanostructures, initially produced via the LAL approach, also exhibited high photocatalytic activity due to their high surface-to-volume ratio and metal/semiconductor interfaces.[173,174] Silicon NPs prepared by using LAL showed promise for environment cleaning applications through the reduction of heavy metal ions such as Cr(VI).[175] Niu et al. developed a one-step LAL-based technique to produce various hollow NPs of metal oxides and sulfides, of which ZnS hollow NPs showed both higher performance in gas sensing and stronger ferromagnetic response than those of ZnS nanocrystals.[36,39] Very recently, the same group deaggregated detonation nanodiamonds by selective laser heating in liquid and found that the magnetic properties of detonated nanodiamonds changed significantly after the deaggregation.[176] In addition, the well-dispersed nanodiamonds covered with organic ligands demonstrated a visible-light emission.[171] Because of the inert features of nanodiamonds, these luminescent nanomaterials are expected to find useful applications in bioimaging and biosensing.[176]

One of typical problems faced in catalytic applications of transition metal NPs is their instability towards aggregation and formation of larger particles, which changes the catalytic properties or even can lead to inactive materials. Higher colloidal stability of LAL produced transition metal NPs solves the issues caused by NP aggregation. Any ionic liquid such as 1-*n*-butyl-3-methylimidazolium hexafluorophosphate (BMI.PF6) can be used as a liquid medium for the generation of stable catalytic NPs using LAL. Gelesky and co-workers[177] performed the laser induced fragmentation of Rh and Pd particles the generate smaller sized and more stable colloidal solutions of NPs. Since all materials suitable for fluorescent, photoconductive, or energy harvesting applications, as well as those used in batteries[178] or as bone implants,[179] can be converted into their NPs via the laser ablation of their pellets or via the laser-induced melting

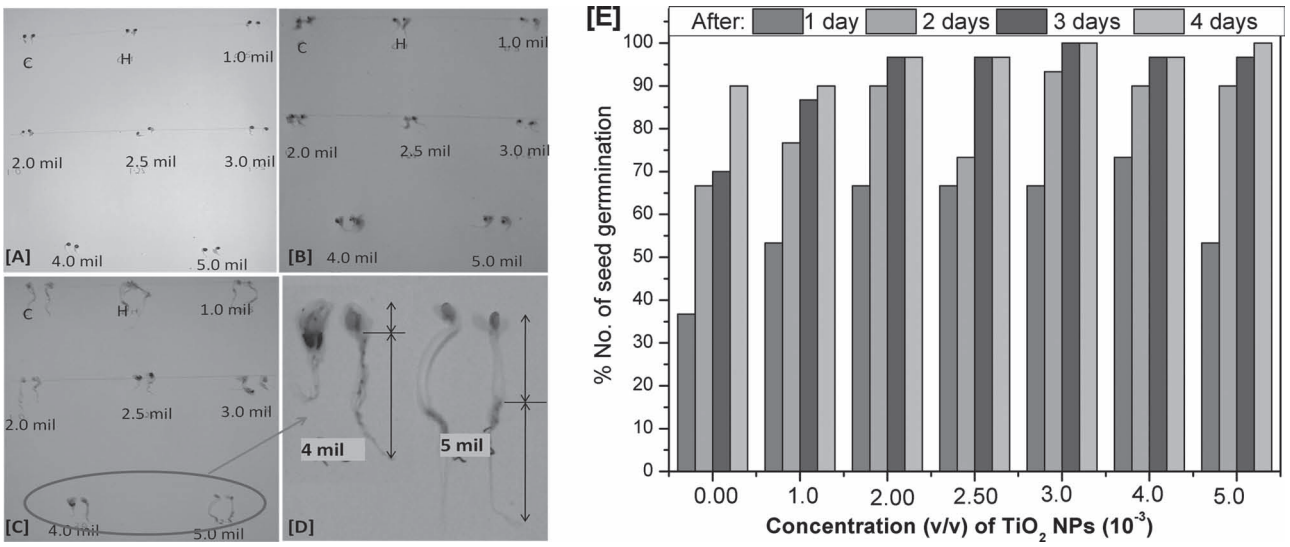

Figure 19. Photographs of TiO_2 treated seed germination A) 3 days, B) 4 days, and C) 5 days of sowing. D) Magnified image of 4 mm (mil) and 5 mm TiO_2 treated *Brassica oleracea* var. *capitata* sees after 5 days of sowing. E] Histogram of percentage of seeds germinated after 1–4 days of sowing for different concentrations of TiO_2 NPs. Reproduced with permission.[172] Copyright 2012, American Scientific Publishers.

and fragmentation of liquid suspended powders, this technique has the potential to prepare nanomaterials for a wide range of applications.

6. Conclusions and Outlook

In this article, we have reviewed the current progress in the field of laser ablation/irradiation and nanostructure preparation in liquid media. According to the literature, besides the investigations on the fundamental mechanisms (such as thermal evaporation, explosive ejection, and photochemical or thermochemical reactions of liquid precursors), several methodologies based on laser ablation in liquid have been recently developed and numerous novel nanostructures have been synthesized. The products include, but are not limited to, metal and alloy nanoparticles; semiconductor and ceramic nanostructures; and metal hydroxide, oxide, sulfide, graphite, and silicon nanostructrures. The size, morphology, and shape of these nanostructures can be controlled by adjusting experimental conditions, including the laser parameters, liquid, and target. Such nanostructures have already exhibited promise for many interesting and important applications in nano-biosurgery, light emission, and SERS.

According to the results reported in this field, the remarkable advantages of LAL and the resulting nanomaterials can be briefly summarized as follows. LAL is a facile, "clean", and rapid synthesis of nanostructures due to the reduced formation of byproducts in the process, simpler precursors, and absence of catalysts. It has very wide versatility regarding diverse nanoproducts, including metals, metal oxides and hydroxides, sulfides, and other materials. This is based on the strong ability of laser to ablate various targets. It is also a method with nominally ambient temperature and pressure conditions to obtain metastable and new-phase nanostructures that may not be attainable by other methods, especially under similar conditions. Furthermore, it is a highly effective method to the one-step and one-pot fabrication of biomolecule-conjugated nanoparticles. As reported, five times more biomolecules may be conjugated to a gold nanoparticle surface produced via this technique. Colloidal solution of metal or semiconductor NPs produced by PLA of corresponding target into desired host polymer/organic matrix can be directly applied for the rapid device fabrication using spin- or dip-coating.[180] Inherent colloidal stability and purity of produced colloidal solution of LAL produced NPs makes them very suitable for biological and medical applications. The main disadvantage of LAL is its low productivity, but with the optimization of ablation and liquid media parameters, gram-scale production can be achieved.[124,125] PLA-generated pure NPs and aggregates provide higher signal-to-noise ratio when used as substrates in SERS.[23]

The achieved results suggest that this technique can represent an attractive field, as well as an indispensable approach for the fabrication of functional nanostructures. However, many unexplored issues in this field are evident, along with the in-depth study. When considering the further research topics, without doubt, studies closely combining the features of LAL with the application demands of various functional materials are necessary and will greatly advance the development of this field. Therefore, in parallel to the further investigations of basic mechanisms of laser ablation/irradiation in liquid, some innovative research efforts are desirable in the future as follows: 1) Methodologies should be further developed, aiming at a narrower size distribution and increased yield of the product. So far, the LAL products demonstrate relatively wide size distributions and low yields, which is not favorable for some applications. 2) For both metal and semiconductor nanoparticles produced using LAL, more isochronous surface modification should be implemented. This will permit the preparation of more new conjugated colloids, which are potentially anticipated

for bioapplications. 3) For semiconductor nanostructures, the preparation of doped and multicomponent semiconductor nanostructures would greatly widen the application range of LAL-generated materials. Such nanomaterials are highly anticipated in catalysis, solar cell electrodes, light-emitting phosphors, etc. Based on the most recent results, this seems feasible though the design of target materials and varying liquid media. 4) Finally, some new routes based on laser irradiation in liquid, aiming at the direct formation of nanopatterns or nanodevices with potential applications in microelectronics, optoelectronics, and biology and medicine, should also attract more attention.

Acknowledgements

This work was supported by the Natural Science Foundation of China (Nos.10604055, 50831005, 50972102, 51171127, and 51041006), and Jiangsu "Jiangsu high-level innovative entrepreneurship talents introduction plan". S.C.S is thankful to the Irish Research Council for Science, Engineering and Technology (IRCSET) for providing an EMPOWER postdoctoral fellowship.

Received: September 26, 2011
Revised: December 19, 2011
Published online: February 6, 2012

[1] T. H. Maiman, *Nature* **1960**, *187*, 493.
[2] M. Hashida, H. Mishima, S. Tokita, S. Sakabe, *Opt. Express* **2009**, *17*, 13116.
[3] S. Chakraborty, H. Sakata, E. Yokoyama, M. Wakaki, D. Chakravorty, *Appl. Surf. Sci.* **2007**, *254*, 638.
[4] H. M. Smith, A. F. Turner, *Appl. Optics* **1965**, *4*, 147.
[5] D. B. Chrisey, G. K. Hubler, *Pulsed Laser Deposition of Thin Films*, John Wiley & Sons, Weinheim **1994.**
[6] A. M. Morales, C. M. Lieber, *Science* **1998**, *279*, 208.
[7] C. Li, D. H. Zhang, S. Han, X. L. Liu, T. Tang, C. W. Zhou, *Adv. Mater.* **2003**, *15*, 143.
[8] Z. Q. Liu, D. H. Zhang, S. Han, C. Li, T. Tang, W. Jin, X. L. Liu, B. Lei, C. W. Zhou, *Adv. Mater.* **2003**, *15*, 1754.
[9] I. Amarilio-Burshtein, S. Tamir, Y. Lifshitz, *Appl. Phys. Lett.* **2010**, *96*, 103014.
[10] R. S. Yang, Y. L. Chueh, J. R. Morber, R. Snyder, L. J. Chou, Z. L. Wang, *Nano. Lett.* **2007**, *7*, 269.
[11] Y. J. Choi, I. S. Hwang, J. H. Park, S. Nahm, J. G. Park, *Nanotechnology* **2006**, *17*, 3775.
[12] R. Savu, E. Joanni, *Scripta Mater.* **2006**, *55*, 979.
[13] Y. F. Zhang, Y. H. Tang, X. F. Duan, Y. Zhang, C. S. Lee, N. Wang, I. Bello, S. T. Lee, *Chem. Phys. Lett.* **2000**, *323*, 180.
[14] B. Eisenhawer, D. Zhang, R. Clavel, A. Berger, J. Michler, S. Christiansen, *Nanotechnology* **2011**, *22*, 075706.
[15] Y. Y. Wu, R. Fan, P. D. Yang, *Nano. Lett.* **2002**, *2*, 83.
[16] J. D. Holmes, K. P. Johnston, R. C. Doty, B. A. Korgel, *Science* **2000**, *287*, 1471.
[17] J. Westwater, D. P. Gosain, S. Tomiya, S. Usui, H. Ruda, *J. Vac. Sci. Technol. B* **1997**, *15*, 554.
[18] X. Duan, C. M. Lieber, *J. Am. Chem. Soc.* **2000**, *122*, 188.
[19] S. C. Singh, H. B. Zeng, *Sci. Adv. Mater.* **2012**, *4* (in press).
[20] A. Fojtik, A. Henglein, B. Bunsen-Ges, *Phys. Chem.* **1993**, *97*, 252.
[21] J. Neddersen, G. Chumanov, T. M. Cotton, *Appl. Spectrosc.* **1993**, *47*, 1959.
[22] A. Pyatenko, K. Shimokawa, M. Yamaguchi, O. Nishimura, M. Suzuki, *Appl. Phys.* **2004**, *79*, 803.
[23] F. Mafune, J. Y. Kohno, Y. Takeda, T. Kondow, *J. Phys. Chem. B* **2000**, *35*, 8335.
[24] F. Mafune, J. Y. Kohno, Y. Takeda, T. Kondow, *J. Phys. Chem. B* **2000**, *104*, 9111.
[25] F. Mafune, J. Y. Kohno, Y. Takeda, T. Kondow, *J. Phys. Chem. B* **2001**, *105*, 5114.
[26] F. Mafune, J. Y. Kohno, Y. Takeda, T. Kondow, *J. Phys. Chem. B* **2002**, *31*, 7577.
[27] F. Mafune, J. Y. Kohno, Y. Takeda, T. Kondow, *J. Phys. Chem. B* **2003**, *107*, 4218.
[28] Y. Takeuchi, T. Ida, K. Kimura, *J. Phys. Chem. B* **1997**, *101*, 1322.
[29] J. P. Sylvestre, A. V. Kabashin, E. Sacher, M. Meunier, J. H. Luong, *J. Am. Chem. Soc.* **2004**, *126*, 7176.
[30] F. Mafune, J. Y. Kohno, Y. Takeda, T. Kondow, *J. Phys. Chem. B* **2001**, *105*, 9050.
[31] F. Mafune, J. Y. Kohno, Y. Takeda, T. Kondow, *J. Am. Chem. Soc.* **2003**, *125*, 1686.
[32] N. Satoh, H. Hasegawa, K. Tsujii, K. Kimura, *J. Phys. Chem. B* **1994**, *98*, 2143.
[33] C. M. Aguirre, C. E. Moran, J. F. Young, N. J. Halas, *J. Phys. Chem. B* **2004**, *108*, 7040.
[34] S. Link, C. Burda, B. Nikoobakht, M. A. E. El-Sayed, *J. Phys. Chem. B* **2000**, *104*, 6152.
[35] J. Bosbach, D. Martin, F. Stietz, T. Wenzel, F. Trager, *Appl. Phys. Lett.* **1999**, *74*, 2605.
[36] K. Y. Niu, J. Yang, S. A. Kulinich, J. Sun, H. Li, X. W. Du, *J. Am. Chem. Soc.* **2010**, *132*, 9814.
[37] K. Y. Niu, J. Yang, J. Sun, X. W. Du, *Nanotechnology* **2010**, *21*, 295604.
[38] F. Lin, J. Yang, S. H. Lu, K. Y. Niu, Y. Liu, J. Sun, X. W. Du, *J. Mater. Chem.* **2010**, *20*, 1103.
[39] K. Y. Niu, J. Yang, S. A. Kulinich, J. Sun, X. W. Du, *Langmuir* **2010**, *26*, 16652.
[40] Q. A. Drmosh, M. A. Gondal, Z. H. Yamani, T. A. Saleh, *Appl. Surf. Sci.* **2010**, *256*, 4661.
[41] P. Liu, Y. L. Cao, H. Cui, X. Y. Chen, G. W. Yang, *Chem. Mater.* **2008**, *20*, 494.
[42] P. Liu, Y. L. Cao, C. X. Wang, X. Y. Chen, G. W. Yang, *Nano. Lett.* **2008**, *8*, 2570.
[43] P. Liu, Y. L. Cao, X. Y. Chen, G. W. Yang, *Cryst. Growth. Des.* **2009**, *9*, 1390.
[44] S. Petersen, S. Barcikowski, *Adv. Funct. Mater.* **2009**, *19*, 1167.
[45] S. Petersen, A. Barchanski, U. Taylor, S. Klein, D. Rath, S. Barcikowski, *J. Phys. Chem. C* **2011**, *115*, 5152.
[46] S. Petersen, S. Barcikowski, *J. Phys. Chem. C* **2009**, *113*, 19830.
[47] S. H. Stelzig, C. Menneking, M. S. Hoffmann, K. Eisele, S. Barcikowski, M. Klapper, K. Muller, *J. Eur. Polym.* **2011**, *47*, 662.
[48] H. B. Zeng, W. Cai, Y. Li, J. Hu, P. Liu, *J. Phys. Chem. B* **2005**, *109*, 18260.
[49] H. B. Zeng, G. Duan, Y. Li, S. Yang, X. Xu, W. Cai, *Adv. Funct. Mater.* **2010**, *20*, 561.
[50] H. B. Zeng, S. Yang, X. Xu, W. Cai, *Appl. Phys. Lett.* **2009**, *95*, 191904.
[51] P. V. Kazakevich, A. V. Simakin, V. V. Voronov, G. A. Shafeev, *Appl. Surf. Sci.* **2006**, *252*, 4373.
[52] G. W. Yang, *Prog. Mater. Sci.* **2007**, *52*, 51.
[53] W. T. Nichols, T. Sasaki, N. Koshizaki, *J. Appl. Phys.* **2006**, *100*, 114911.
[54] W. T. Nichols, T. Sasaki, N. Koshizaki, *J. Appl. Phys.* **2006**, *100*, 114912.
[55] W. T. Nichols, T. Sasaki, N. Koshizaki, *J. Appl. Phys.* **2006**, *100*, 114913.

[56] T. Sakka, S. Iwanaga, Y. H. Ogata, A. Matsunawa, T. Takemoto, *J. Chem. Phys.* **2000**, *112*, 8645.
[57] L. Yang, P. W. May, L. Yin, J. A. Smith, K. N. Rosser, *J. Nanopart. Res.* **2007**, *9*, 1181.
[58] R. K. Thareja, S. Shukla, *Appl. Surf. Sci.* **2007**, *253*, 8889.
[59] P. S. Liu, W. P. Cai, H. B. Zeng, *J. Phys. Chem. C* **2008**, *112*, 3261.
[60] H. B. Zeng, Z. Li, W. Cai, B. Cao, P. Liuand, S. Yang, *J. Phys. Chem. B* **2007**, *111*, 14311.
[61] H. B. Zeng, X. Xu, Y. Bando, U. K. Gautam, T. Zhai, X. Fang, B. Liu, D. Golberg, *Adv. Funct. Mater.* **2009**, *19*, 3165.
[62] Q. X. Liu, C. X. Wang, G. W. Yang, *Eur. Phys. B* **2004**, *41*, 479.
[63] A. V. Simakin, V. V. Voronov, N. A. Kirichenko, G. A. Safeev, *Appl. Phys. A* **2004**, *79*, 1127.
[64] T. Tsuji, Y. Tsuboi, N. Kitamura, M. Tsuji, *Appl. Surf. Sci.* **2004**, *229*, 365.
[65] J. H. Yoo, S. H. Jeong, R. Greif, R. E. Russo, *J. Appl. Phys.*, **2000**, *88*, 1638.
[66] T. X. Phuoc, B. H. Howard, D. V. Martello, Y. Soong, M. K. Chu, *Opt. Lasers Eng.* **2008**, *46*, 829.
[67] D. Werner, S. Hashimoto, *J. Phys. Chem. C* **2011**, *115*, 5063.
[68] A. Pyatenko, M. Yamaguchi, M. Suzuki, *J. Phys. Chem. C* **2009**, *113*, 9078.
[69] S. C. Singh, S. K. Mishra, R. K. Srivastava, R. Gopal, *J. Phys. Chem. C* **2010**, *114*, 17374.
[70] H. B. Zeng, S. Yang, W. Cai, *J. Phys. Chem. C* **2011**, *115*, 5038.
[71] F. Mafune, J. Kohno, Y. Takeda, T. Kondow, *J. Phys. Chem. B* **2003**, *107*, 12589.
[72] a) P. V. Kamat, M. Flumiani, G. V. Hartland, *J. Phys. Chem. B* **1998**, *102*, 3123; b) H. Fujiwara, S. Yanagida, P. V. Kamat, *J. Phys. Chem. B* **1999**, *103*, 2589.
[73] A. Giusti, E. Giorgetti, S. Laza, P. Marsili, F. Giammanco, *J. Phys. Chem. C* **2007**, *111*, 14984.
[74] K. Yamada, Y. Tokumoto, T. Nagata, F. Mafune, *J. Phys. Chem. B* **2006**, *110*, 11751.
[75] H. Muto, K. Miyajima, F. Mafune, *J. Phys. Chem. C* **2008**, *112*, 5810.
[76] J. Zhang, J. Worley, S. Denommee, C. Kingston, Z. J. Jakubek, Y. Deslandes, M. Post, B. Simard, *J. Phys. Chem. B* **2003**, *107*, 6920.
[77] H. Hada, Y. Yonezawa, A. Yoshida, A. Kurakake, *J. Phys. Chem.* **1976**, *80*, 2728.
[78] K. Kurihara, J. Kizling, P. Stenius, J. H. Fendler, *J. Am. Chem. Soc.* **1983**, *105*, 2574.
[79] S. Eustis, H.Y. Hsu, M.A. El-Sayed, *J. Phys. Chem. B* **2005**, *109*, 4811.
[80] B. Marciniak, G.E. Buono-Core, *J. Photochem. Photobiol. A* **1990**, *52*, 1.
[81] M. Sakamoto, M. Fujistuka, T. Majima, *J. Photochem. Photobiol. C: Photochem. Rev.* **2009**, *10*, 33.
[82] M. Sakamoto, T. Tachikawa, M. Fujitsuka, T. Majima, *Langmuir* **2006**, *22*, 6361.
[83] B. Kraeutler, A. J. Bard, *J. Am. Chem. Soc.* **1978**, *100*, 4317.
[84] A. J. Bard, M. A. Fox, *Acc. Chem. Res.* **1995**, *28*, 141.
[85] P.V. Kamat, *J. Phys. Chem. B* **2002**, *106*, 7729.
[86] S. J. Tauster, S. C. Fung, R. L. Garten, *J. Am. Chem. Soc.* **1978**, *100*, 170.
[87] P. D. Fleischauer, H. K. A. Kan, J. R. Shepard, *J. Am. Chem. Soc.* **1972**, *94*, 283.
[88] H. Hada, Y. Yonezawa, M. Saikawa, *J. Chem. Soc., Faraday Trans.* **1982**, *26*, 2677.
[89] H. Hada, Y. Yonezawa, M. Saikawa, *Bull. Chem. Soc. Jpn.* **1982**, *55*, 2010.
[90] A. Wood, M. Giersig, P. Mulvaney, *J. Phys. Chem. B* **2001**, *105*, 8810.
[91] K. Siskova, B. Vlckova, P. Y. Turpin, A. Thorel, M. Prochazka, *J. Phys. Chem. C* **2011**, *115*, 5404.
[92] S. Yang, W. Cai, G. Liu, H. Zeng, *J. Phys. Chem. C* **2009**, *113*, 7692.
[93] K. Siskova, B. Vlckova, P.-Y. Turpin, C. Fayet, *J. Phys. Chem. C* **2008**, *112*, 4435.
[94] V. Amendola, S. Polizzi, M. Meneghetti, *Langmuir* **2007**, *23*, 6766.
[95] S. C. Singh, R. Gopal, *Bull. Mater. Sci.* **2007**, *30*, 291.
[96] X. Zhang, H. B. Zeng, W. Cai, *Mater. Lett.* **2009**, *63*, 191.
[97] S. C. Singh, R. K. Swarnkar, R. Gopal, *Bull. Mater. Sci.* **2010**, *33*, 21.
[98] S. I. Dolgaev, A. V. Simakin, V. V. Voronov, G. A. Safeev, F. Bozon-Verduraz, *Appl. Surf. Sci.* **2002**, *186*, 546.
[99] A. Baladi, R. S. Mamoory, *Appl. Surf. Sci.* **2010**, *256*, 7559.
[100] J. Jhang, C. Q. Lan, *Mater. Lett.* **2008**, *62*, 1521.
[101] S. Kima, B. K. Yooa, K. Chuna, W. Kanga, J. Choob, M.-S. Gongc, S.-W. Jooa, *J. Mol. Catal. A: Chem.* **2005**, *226*, 231.
[102] M. S. F. Lima, F. P. Ladário, R. Riva, *Appl. Surf. Sci.* **2006**, *252*, 4420.
[103] S. C. Singh, *J. Nanopart. Res.* **2011**, *13*, 4143.
[104] S. C. Singh, R. Gopal, *Appl. Surf. Sci.* **2012**, 258, 2211.
[105] S. C. Singh, R. Gopal, *J. Phys. Chem. C* **2008**, *112*, 2812.
[106] S. C. Singh, R. Gopal, *Physica E* **2008**, *40*, 724.
[107] S. C. Singh, R. K. Swarnkar, R. Gopal, *J. Nanosci. Nanotechnol.* **2009**, *9*, 5367.
[108] A. S. Nikolov, P. A. Atanasov, D. R. Milev, T. R. Stoyanchov, A. D. Deleva, Z. Y. Peshev, *Appl. Surf. Sci.* **2009**, *255*, 5351.
[109] C.-N. Huang, J.-S. Bow, Y. Zheng, S.-Y. Chen, N. J. Ho, P. Shen, *Nanoscale Res. Lett.* **2010**, *5*, 972.
[110] N. Takada, T. Sasaki, K. Sasaki, *Appl. Phys. A* **2008**, *93*, 833.
[111] J. S. Golightly, A. W. Castleman, *J. Phys. Chem. B* **2006**, *110*, 19979.
[112] S. C. Singh, R. K. Swarnkar, R. Gopal, *J. Nanopart. Res.* **2009**, *11*, 1831.
[113] S. C. Singh, R. Gopal, *J. Phys. Chem. C* **2010**, *114*, 9277.
[114] C. Liang, Y. Shimizu, M. Masuda, T. Sasaki, N. Koshizaki, *Chem. Mater.* **2004**, *16*, 963.
[115] H. Usui, T. Sasaki, N. Koshizaki, *Chem. Lett.* **2005**, *34*, 700.
[116] H. Usui, T. Sasaki, N. Koshizaki, *Chem. Lett.* **2006**, *35*, 752.
[117] Z. Yan, R. Bao, D. B. Chrisey, *Chem. Phys. Lett.* **2010**, *497*, 205.
[118] Z. Yan, G. Compagnini, D. B. Chrisey, *J. Phys. Chem. C* **2011**, *115*, 5058.
[119] Z. Yan, R. Bao, D. B. Chrisey, *Langmuir* **2011**, *27*, 851.
[120] D. C. Schinca, L. B. Scaffardi, F. A. Videla, G. A. Torchia, P. Moreno, L. Roso, *J. Phys. D* **2009**, *42*, 215102.
[121] C. He, T. Sasaki, Y. Zhou, Y. Shimizu, M. Masuda, N. Koshizaki, *Adv. Funct. Mater.* **2007**, *17*, 3554.
[122] M. Kawasaki, *J. Phys. Chem. C* **2011**, *115*, 5165.
[123] M.-S. Yeh, Y.-S. Yang, Y.-P. Lee, H.-F. Lee, Y.-H. Yeh, C.-S. Yeh, *J. Phys. Chem. B* **1999**, *103*, 6851.
[124] Y.-H. Chen, C.-S. Yeh, *Chem. Commun.* **2001**, 371.
[125] Y. Yonezawa, T. Sato, S. Kuroda, K. Kuge, *J. Chem. Soc., Faraday Trans.* **1991**, *87*, 1905.
[126] N. Kometani, H. Doi, K. Asami, Y. Yonezawa, *Phys. Chem. Chem. Phys.* **2002**, *4*, 5142.
[127] A. Henglein, *Chem. Mater.* **1998**, *10*, 444.
[128] P. Liu, C. Wang, X. Chen, G. Yang, *J. Phys. Chem. C* **2008**, *112*, 13450.
[129] C. Sajti, R. Sattari, B. Chichkov, S. Barcikowski, *J. Phys. Chem. C* **2010**, *114*, 2421.
[130] P. Wagener, A. Schwenke, B. Chichkov, S. Barcikowski, *J. Phys. Chem. C* **2010**, *114*, 7618.
[131] S. I. Dolgaev, A. V. Simakin, V. V. Voronov, G. A. Shafeev, F. Bozon-Verduraz, *Appl. Surf. Sci.* **2002**, *186*, 546.
[132] J. Sun, S. L. Hu, X. W. Du, Y. W. Lei, L. Jiang, *Appl. Phys. Lett.* **2006**, *89*, 183115.
[133] G. Cristoforetti, E. Pitzalis, R. Spiniello, R. Ishak, M. Muniz-Miranda, *J. Phys. Chem. C* **2011**, *115*, 5073.

[134] M. Muniz-Miranda, C. Gellini, E. Giorgetti, *J. Phys. Chem. C* **2011**, *115*, 5021.
[135] P. P. Patil, D. M. Phase, S. A. Kulkarni, S. V. Ghaisas, S. K. Kulkarni, S. M. Kanetkar, S. B. Ogale, V. G. Bhide, *Phys. Rev. Lett.* **1987**, *58*, 238.
[136] H. M. Zhang, C. H. Liang, Z. F. Tian, G. Z. Wang, W. P. Cai, *J. Phys. Chem. C* **2010**, *114*, 12524.
[137] K. Jayawardena, J. Fryar, S. Ravi, P. Silva, S. J. Henley, *J. Phys. Chem. C* **2010**, *114*, 12931.
[138] C. Fauteux, R. Longtin, J. Pegna, D. Therriault, *Inorg. Chem.* **2007**, *46*, 11036.
[139] K. Kordas, J. Bekesi, R. Vajtai, L. Nanai, S. Leppavuori, A. Uusimaki, K. Bali, T. F. George, G. Galbacs, F. Ignacz, P. Moilanen, *Appl. Surf. Sci.* **2001**, *172*, 178.
[140] Z. Geretovszky, T. Szörényi, *Appl. Surf. Sci.* **1997**, *467*, 109.
[141] H. B. Zeng, C. Zhi, Z. Zhang, X. Wei, X. Wang, W. Guo, Y. Bando, D. Golberg, *Nano. Lett.* **2010**, *10*, 5049.
[142] X. W. Du, W. J. Qin, Y. W. Lu, X. Han, Y. S. Fu, S. L. Hu, *J. Appl. Phys.* **2007**, *102*, 013518.
[143] F. Tian, J. Sun, J. Yang, P. Wu, H. L. Wang, X. W. Du, *Mater. Lett.* **2009**, *63*, 2384.
[144] S. L. Hu, J. Sun, X. W. Du, F. Tian, L. Jiang, *Diamond Relat. Mater.* **2008**, *17*, 142.
[145] F. Hajiesmaeilbaigi, A. Motamedi, M. Ruzbehani, *Laser Phys.* **2010**, *20*, 508.
[146] G. Bajaj, R. K. Soni, *J. Nanopart. Res.* **2010**, *12*, 2597.
[147] E. Jimenez, K. Abderrafi, R. Abargues, J. L. Valdes, J. P. Martinez-Pastor, *Langmuir* **2010**, *26*, 7458.
[148] N. Shirahata, M. R. Linford, S. Furumi, L. Pei, Y. Sakka, R. J. Gates, M. C. Asplund, *Chem. Commun.* **2009**, 4684.
[149] S. L. Hu, K. Y. Niu, J. Sun, J. Yang, N. Q. Zhao, X. W. Du, *J. Mater. Chem.* **2009**, *19*, 484.
[150] J. B. Park, S. H. Jeong, M. S. Jeong, J. Y. Kim, B. K. Cho, *Carbon* **2008**, *46*, 1369.
[151] S. Mollah, *Asian J. Chem.* **2009**, *21*, 1.
[152] X. Z. Lin, P. Liu, J. M. Yu, G. W. Yang, *J. Phys. Chem. C* **2009**, *113*, 17543.
[153] J. Sylvestre, A. V. Kabashin, E. Sacher, M. Meunier, J. H. T. Luong, *J. Am. Chem. Soc.* **2004**, *126*, 7176.
[154] S. Salmaso, P. Caliceti, V. Amendola, M. Meneghetti, J. P. Magnusson, G. Pasparakis, C. Alexander, *J. Mater. Chem.* **2009**, *19*, 1608.
[155] J. G. Walter, S. Petersen, F. Stahl, T. Scheper, S. Barcikowski, *J. Nanobiotechnol.* **2010**, *8*, 21.
[156] X. L. Cao, H. B. Zeng, M. Wang, X. Xu, M. Fang, S. Ji, L. D. Zhang, *J. Phys. Chem. C* **2008**, *112*, 5267.
[157] H. B. Zeng, P. Liu, W. Cai, X. Cao, S. Yang, *Cryst. Growth Des.* **2007**, *7*, 1092.
[158] H. B. Zeng, W. Cai, J. Hu, G. Duan, P. Liu, Y. Li, *Appl. Phys. Lett.* **2006**, *88*, 171910.
[159] B. Cao, W. Cai, H. B. Zeng, *Appl. Phys. Lett.* **2006**, *88*, 161101.
[160] M. Chang, H. B. Zeng, X. L. Cao, *J. Phys. Chem. C* **2009**, *113*, 15544.
[161] H. B. Zeng, J. B. Cui, B. Q. Cao, U. Gibson, Y. Bando, D. Golberg, *Sci. Adv. Mater.* **2010**, *2*, 336.
[162] H. B. Zeng, Z. Li, W. Cai, P. Liu, *J. Appl. Phys.* **2007**, *102*, 10437.
[163] H. B. Zeng, W. Cai, B. Cao, J. Hu, Y. Li, P. Liu, *Appl. Phys. Lett.* **2006**, *88*, 181905.
[164] S. Yang, H. B. Zeng, H. Zhao, H. Zhang, W. Cai, *J. Mater. Chem.* **2011**, *21*, 4432.
[165] S. Yang, W. Cai, H. Zhang, X. Xu, H. B. Zeng, *J. Phys. Chem. C* **2009**, *113*, 19091.
[166] S. Yang, W. Cai, H. B. Zeng, Z. Li, *J. Appl. Phys.* **2008**, *104*, 023516.
[167] S. Ledoux, D. Amans, C. Dujardin, K. Masenelli-Varlot, *Nanotechnology* **2009**, *20*, 445605.
[168] M. Prochazka, P. Mojzes, J. Stepanek, B. Vlckova, P.-Y. Turpin, *Anal. Chem.* **1997**, *69*, 5103.
[169] S. Yang, W. Cai, L. Kong, Y. Lei, *Adv. Funct. Mater.* **2010**, *20*, 2527.
[170] A. Besner, M. Meunier, *J. Phys. Chem. C* **2010**, *114*, 10403.
[171] P. Liu, W. Cai, M. Fang, Y. Li, H. B. Zeng, J. Hu, X. Luo, W. Jing, *Nanotechnology* **2009**, *20*, 285707.
[172] D. Singh, S. Kumar, S. C. Singh, B. Lal, N. B. Singh, *Sci. Adv. Mater.* **2012**, **4** (in press).
[173] H. B. Zeng, P. Liu, W. Cai, S. Yang, X. Xu, *J. Phys. Chem. C* **2008**, *112*, 19620.
[174] H. B. Zeng, W. Cai, P. Liu, X. Xu, H. Zhou, C. Klingshirn, H. Kalt, *ACS Nano* **2008**, *2*, 1661.
[175] S. Yang, W. Cai, G. Liu, H. B. Zeng, P. Liu, *J. Phys. Chem. C* **2009**, *113*, 6480.
[176] K. Y. Niu, H. M. Zheng, Z. Q. Li, J. Yang, J. Sun, X. W. Du, *Angew. Chem. Int. Ed.* **2011**, *123*, 4185.
[177] M. A. Gelesky, A. P. Umpierre, G. Machado, R. R. B. Correia, W. C. Magno, J. Morais, G. Ebeling, J. Dupont, *J. Am. Chem. Soc.* **2005**, *127*, 4588.
[178] T. Tsuji, Y. Tatsuyama, M. Tsuji, K. Ishida, S. Okada, J. Yamaki, *Mater. Lett.* **2007**, *61*, 2062.
[179] O. R. Musaev, V. Dusevich, D. M. Wieliczka, J. M. Wrobel, M. B. Kruger, *J. Appl. Phys.* **2008**, *104*, 084316.
[180] V. Svrcek, D. Mariotti, T. Nagai, Y. Shibata, I. Turkevych, M. Kondo, *J. Phys. Chem. C* **2011**, *115*, 5084.